USGS
science for a changing world

Prepared in cooperation with the San Francisco Bay Regional Water Quality Control Board and Bay Area Clean Water Agencies

A Tidally Averaged Sediment Transport Model for San Francisco Bay, California

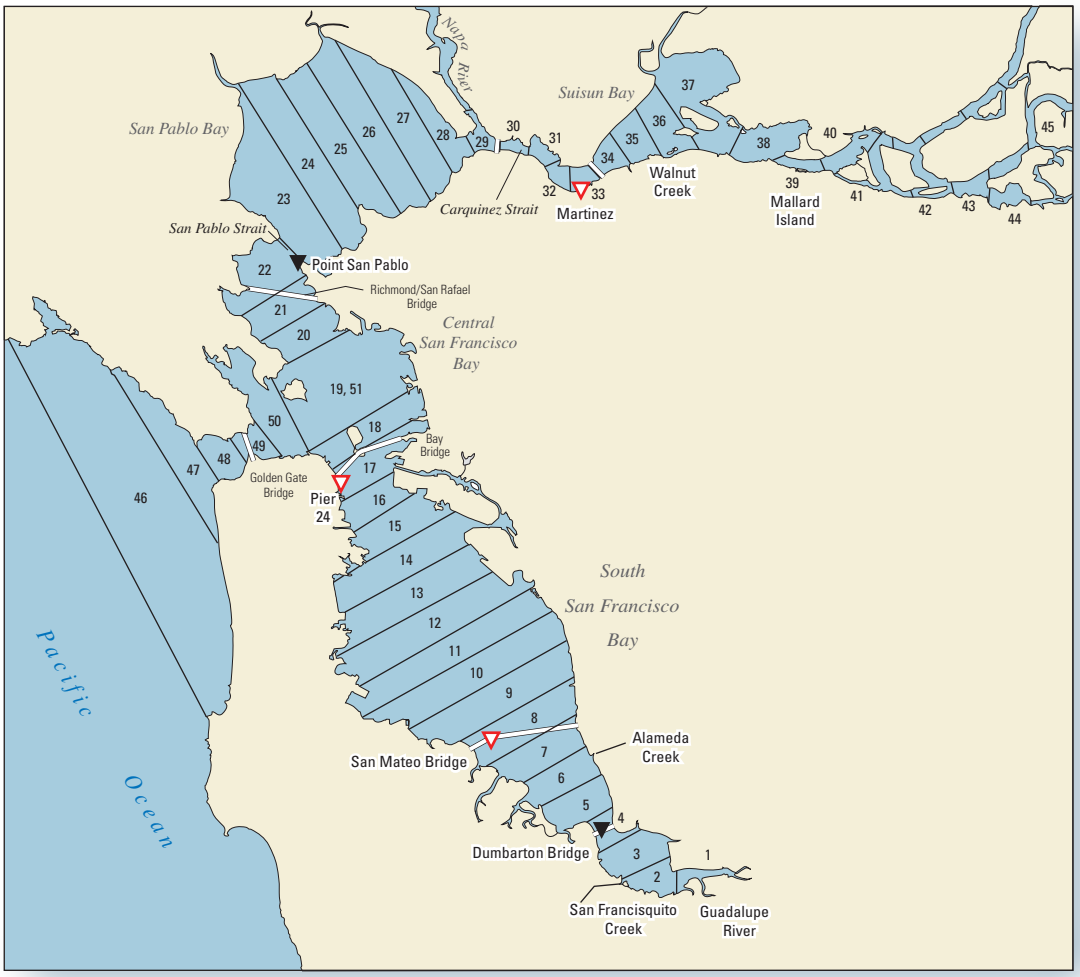

Scientific Investigations Report 2009-5104

U.S. Department of the Interior
U.S. Geological Survey

A Tidally Averaged Sediment-Transport Model for San Francisco Bay, California

By Megan A. Lionberger and David H. Schoellhamer

Prepared in cooperation with the San Francisco Bay Regional Water Quality Control Board and the Bay Area Clean Water Agencies

Scientific Investigations Report 2009–5104

U.S. Department of the Interior
U.S. Geological Survey

U.S. Department of the Interior
KEN SALAZAR, Secretary

U.S. Geological Survey
Suzette M. Kimball, Acting Director

U.S. Geological Survey, Reston, Virginia: 2009

For more information on the USGS—the Federal source for science about the Earth, its natural and living resources, natural hazards, and the environment, visit *http://www.usgs.gov* or call 1-888-ASK-USGS

For an overview of USGS information products, including maps, imagery, and publications, visit *http://www.usgs.gov/pubprod*

To order this and other USGS information products, visit *http://store.usgs.gov*

Suggested citation:
Lionberger, M.A., and Schoellhamer, D.H., 2009, A tidally averaged sediment-transport model for San Francisco Bay, California: U.S. Geological Survey Scientific Investigations Report 2009–5104, 24 p.

Contents

Abstract 1
Introduction 2
    Purpose and Scope 2
    Description of the Study Area 3
Uncles–Peterson Salinity Model 4
    Mixing Processes 5
    Salinity Model Validation 6
    Applications of the Uncles–Peterson Salinity Model 6
Sediment-Transport Model 7
    Input Data 7
    Suspended-Sediment Concentration Boundary Conditions 11
    Suspended-Sediment Algorithm 11
    Sediment-Bed Algorithm 13
    Model Calibration 14
    Model Validation 14
    Sensitivity Analysis 17
    User's Guide 18
    Applications of the Sediment-Transport Model 18
Conclusions 19
Acknowledgments 19
References Cited 19
Appendix 24

Figures

Figure 1. Uncles–Peterson salinity model segmentation of San Francisco Bay, California, and locations of U.S. Geological Survey continuous salinity monitoring sites.....3
Figure 2. Sample model segment composed of an upper and lower layer.....5
Figure 3. Time series of salinity model validation of (*A*) near-surface and (*B*) near-bottom at Martinez, North San Francisco Bay, California, water year 1999. 7
Figure 4. Time series of salinity model validation of (*A*) near-surface and (*B*) near-bottom at Pier 24, Central San Francisco Bay, California, water year 1999 8
Figure 5. Time series of salinity model validation of (*A*) near-surface and (*B*) near-bottom at San Mateo Bridge, South San Francisco Bay, California, water year 1999 9
Figure 6. Comparison of suspended-sediment flux measured by McKee and others (2006) and predicted by equation 9. 10
Figure 7. Daily mean squared wind speed for North Bay and South Bay used when hourly wind data are unavailable 10
Figure 8. Time series of (*A*) mid-depth and (*B*) near-bottom measured (red) and simulated (blue) suspended-sediment concentrations at Point San Pablo, San Pablo Bay, California, water year 1999. 15
Figure 9. Time series of (*A*) mid-depth and (*B*) near-bottom measured (red) and simulated (blue) suspended-sediment concentrations at Dumbarton Bridge, South San Francisco Bay, California, water year 1999.....16
Figure 10. Time series of upper-layer (red) and lower-layer (blue) bed elevation change for box 5, for a simulation run from January 1, 1940, to September 30, 2002 17

Tables

Table 1. Land subsidence rates in boxes 1-4 for 1934-60, 1960-67, and 1967–82 11
Table 2. Summary of tributary sediment loads (Porterfield, 1980) and Uncles–Peterson box distribution 12
Table 3. Estimated net sedimentation change based on bathymetric survey analysis and net sedimentation calculated by the sediment-transport model calibrated to suspended-sediment concentrations 16
Table 4. Validation of Uncles–Peterson sediment model calibrated to net sedimentation for South San Francisco Bay, California, 1983–2004 17
Table 5. Percent change in suspended-sediment concentration, relative to a 20-percent increase of each calibration coefficient for the sediment model calibrated to suspended-sediment concentrations 18
Table 6. Percent change in net sedimentation, relative to a 20-percent increase of each calibration coefficient for the sediment model calibrated to net sedimentation 18
Table A1. Calibration coefficients for the sediment-transport model calibrated to suspended-sediment concentration.....24
Table A2. Calibration coefficients for the sediment-transport model calibrated to net change in sediment storage 24

Conversion Factors

SI to Inch/Pound

Multiply	By	To obtain
	Length	
centimeter (cm)	0.3937	inch (in.)
meter (m)	3.281	foot (ft)
kilometer (km)	0.6214	mile (mi)
	Area	
square kilometer (km^2)	247.1	acre
square meter	10.76	square foot (ft^2)
	Flow rate	
cubic meter per second	35.31	cubic foot per second (ft^3/s)
meter per second (m/s)	3.281	foot per second (ft/s)
millimeter per year (mm/yr)	0.03937	inch per year (in/yr)
	Mass	
metric ton per day	1.102	ton per day (ton/d)
megatonnes (Mt)	1102000.	ton, short (2,000 lb)
	Pressure and shear stress	
kilogram per cubic meter	0.06242	pound per cubic foot (lb/ft^3)
Newton per square meter (N/m^2)	0.02089	pound per square foot (lb/ft^2)
	Longitudinal dispersion coefficient and eddy diffusivity	
square meters per second (m^2/s)	10.76	square feet per second (ft^2/s)
	Erosion and deposition rate	
grams per square meter per second [$(g/m^2)/s$]	0.000205	pounds per square foot per second [$(lb/ft^2)/s$]

Temperature in degrees Celsius (°C) may be converted to degrees Fahrenheit (°F) as follows:

$$°F=(1.8×°C)+32$$

Temperature in degrees Fahrenheit (°F) may be converted to degrees Celsius (°C) as follows:

$$°C=(°F-32)/1.8$$

Concentrations of chemical constituents in water are given in milligrams per liter (mg/L).

Abbreviations and Acronyms

BDWM	Bay–Delta watershed model
Delta	Sacramento–San Joaquin River Delta
SSC	suspended-sediment concentration
TMDL	total maximum daily load
UP	Uncles–Peterson salinity model

A Tidally Averaged Sediment-Transport Model for San Francisco Bay, California

By Megan A. Lionberger and David H. Schoellhamer

Abstract

A tidally averaged sediment-transport model of San Francisco Bay was incorporated into a tidally averaged salinity box model previously developed and calibrated using salinity, a conservative tracer (Uncles and Peterson, 1995; Knowles, 1996). The Bay is represented in the model by 50 segments composed of two layers: one representing the channel (>5-meter depth) and the other the shallows (0- to 5-meter depth). Calculations are made using a daily time step and simulations can be made on the decadal time scale.

The sediment-transport model includes an erosion-deposition algorithm, a bed-sediment algorithm, and sediment boundary conditions. Erosion and deposition of bed sediments are calculated explicitly, and suspended sediment is transported by implicitly solving the advection-dispersion equation. The bed-sediment model simulates the increase in bed strength with depth, owing to consolidation of fine sediments that make up San Francisco Bay mud. The model is calibrated to either net sedimentation calculated from bathymetric-change data or measured suspended-sediment concentration. Specified boundary conditions are the tributary fluxes of suspended sediment and suspended-sediment concentration in the Pacific Ocean.

Results of model calibration and validation show that the model simulates the trends in suspended-sediment concentration associated with tidal fluctuations, residual velocity, and wind stress well, although the spring neap tidal suspended-sediment concentration variability was consistently underestimated. Model validation also showed poor simulation of seasonal sediment pulses from the Sacramento–San Joaquin River Delta at Point San Pablo because the pulses enter the Bay over only a few days and the fate of the pulses is determined by intra-tidal deposition and resuspension that are not included in this tidally averaged model.

The model was calibrated to net-basin sedimentation to calculate budgets of sediment and sediment-associated contaminants. While simulated net sedimentation in the four basins that comprise San Francisco Bay was correct, the simulations incorrectly eroded shallows while channels deposited because model surface-layer boxes span both shallows and channels, and neglect lateral variability of suspended-sediment concentration. Validation with recent (1983–2005) net sedimentation in South San Francisco Bay was poor, perhaps owing to poorly quantified sediment supply, and to invasive species that altered erosion and deposition processes. This demonstrates that deterministically predicting future sedimentation is difficult in this or any estuary for which boundary conditions are not stationary. The model would best be used as a tool for developing past and present sediment budgets, and for creating scenarios of future sedimentation that are compared to one another rather than considered a deterministic prediction.

Introduction

Section 303(d) of the Federal Clean Water Act requires states to establish a total maximum daily load (TMDL) of a contaminant that is allowed to be discharged to a water body when a contaminant water-quality objective is not met (Schoellhamer and others, 2007). Development of a TMDL requires quantitative knowledge of the mass budget of a contaminant, its sources and sinks, and the resulting levels in fish, sediment, and water. Allocation and implementation of the TMDL requires understanding of the relative importance, the ability to control sources, and the ability to evaluate the effect of management actions and controls on contaminant levels in the Bay. Some contaminants associate with sediment and, thus, their fate in the environment is determined by the fate of sediment (Schoellhamer and others, 2007). Several trace metals and hydrophobic organic chemicals of environmental concern primarily are associated with particulate organic matter and sediments in aquatic systems largely due to processes of adsorption onto mineral surfaces, absorption into organic matter, ion-exchange, and salting-out effects in estuarine environments (Turner and Millward, 2002). Accordingly, suspended sediment moving into, within, and out of estuaries, provides a pathway for the transport of sediment-associated contaminants (Turner and others, 1999; Turner and Millward, 2000; Bergamaschi and others, 2001; and Le Roux and others, 2001). Over time, deposition of contaminated suspended sediment on the bottom creates reservoirs of contaminants in many estuaries (Ridgeway and Shimmield, 2002; and Taylor and others, 2004), including San Francisco Bay (Hornberger and others, 1999; and Venkatesan and others, 1999). Subsequent erosion of bottom sediment can remobilize previously buried contaminants (Hornberger and others, 1999; Lee and Cundy, 2001; and Arzayus and others, 2002), which potentially contributes to contamination of the overlying water column (Turner and Millward, 2002; and Conaway and others, 2003). This is of particular concern for many legacy contaminants (for example, the pesticide, DDT) that no longer are supplied to an estuary in large quantities, compared to historic inputs, but continue to persist because the bottom sediment acts as a source, as in the case of San Francisco Bay.

Sediment dynamics in San Francisco Bay are an important factor affecting the transport and fate of hydrophobic organic contaminants (Venkatesan and others, 1999; Bergamaschi and others, 2001; Ross and Oros, 2004; and Oros and others, 2005), mercury (Choe and others, 2003; and Conaway and others, 2003), and other trace metals (Sanudo-Wilhelmy and others, 1996; Hornberger and others, 1999; and Schoellhamer and others, 2007). For sediment-associated contaminants, the contaminant mass budget and contaminant transport and fate are linked strongly to the Bay sediment budget. Monitoring and modeling of sediment transport in the system are critical for TMDL development and implementation.

Several projects that would restore diked baylands to tidal marsh are being planned in San Francisco Bay. One effect of breaching a pond to a tidal slough or Bay is to increase the tidal prism of the slough and Bay. Tidal prism is the change in water volume between low and high tide for a given region. If the tidal prism increases, then tidal velocities must increase. Increased velocity can cause erosion in the slough and in the Bay (Swanson and others, 2003). This erosion may cause loss of existing marsh or tidal flats. For example, the marshes in the Medway Estuary, England, were enclosed by levees beginning about 1700, but were breached by tides in the 1880s. Recently, the marshes have been accreting while the salt marsh creeks and cliffs and tidal flats have eroded (Kirby, 1990). Restoration essentially undoes what was done with the original diking of the tidal marsh: reduce tidal prism and allow remaining tidal channels to fill with sediment (Hood, 2004). In San Francisco Bay, wetland restoration is potentially limited by sediment supply and sea level rise, A numerical model of sediment transport and net sedimentation would assist with planning restoration projects in San Francisco Bay.

Purpose and Scope

This report describes a tidally averaged sediment-transport model for San Francisco Bay. The model was developed by adding algorithms to the existing Uncles–Peterson (UP) (1995) salinity model to simulate sediment transport in San Francisco Bay on a decadal time scale. The UP model uses a daily time step and represents the Bay with 50 segments composed of 2 layers, one representing the channel (greater than 5 meter- [m] depth) and the other the shallows (0 to 5-m depth). The sediment-transport model was incorporated into the UP model because the hydrodynamics of the model segments have been defined and previously calibrated with salinity, a conservative tracer. The salinity model has been distributed widely and used in other studies to simulate the effects of climate on salinity in San Francisco Bay (Knowles, 2002; Knowles and Cayan, 2002; Uncles, 2003; and Knowles and Cayan, 2004).

The sediment-transport model, described in this report, includes algorithms for erosion and deposition, and a sediment bed algorithm. Boundary conditions are required at Mallard Island, the Pacific Ocean, and five major tributaries (Walnut Creek, Napa River, Alameda Creek, San Francisquito Creek, and Guadalupe River) (*fig. 1*). The model can be calibrated to either daily average suspended-sediment concentration (SSC) or net decadal sedimentation, but not both simultaneously. A numerical sediment-transport model calibrated to SSC cannot be used to accurately simulate net sedimentation because small errors compound over longer simulation periods (Schoellhamer and others, 2008). Two separate calibrations are presented in this report, one to SSC and a second to net sedimentation. Validation of the model calibrated to SSC is given by Lionberger (2003). Validation of the model calibrated to net sedimentation and a sensitivity analysis are presented in this report.

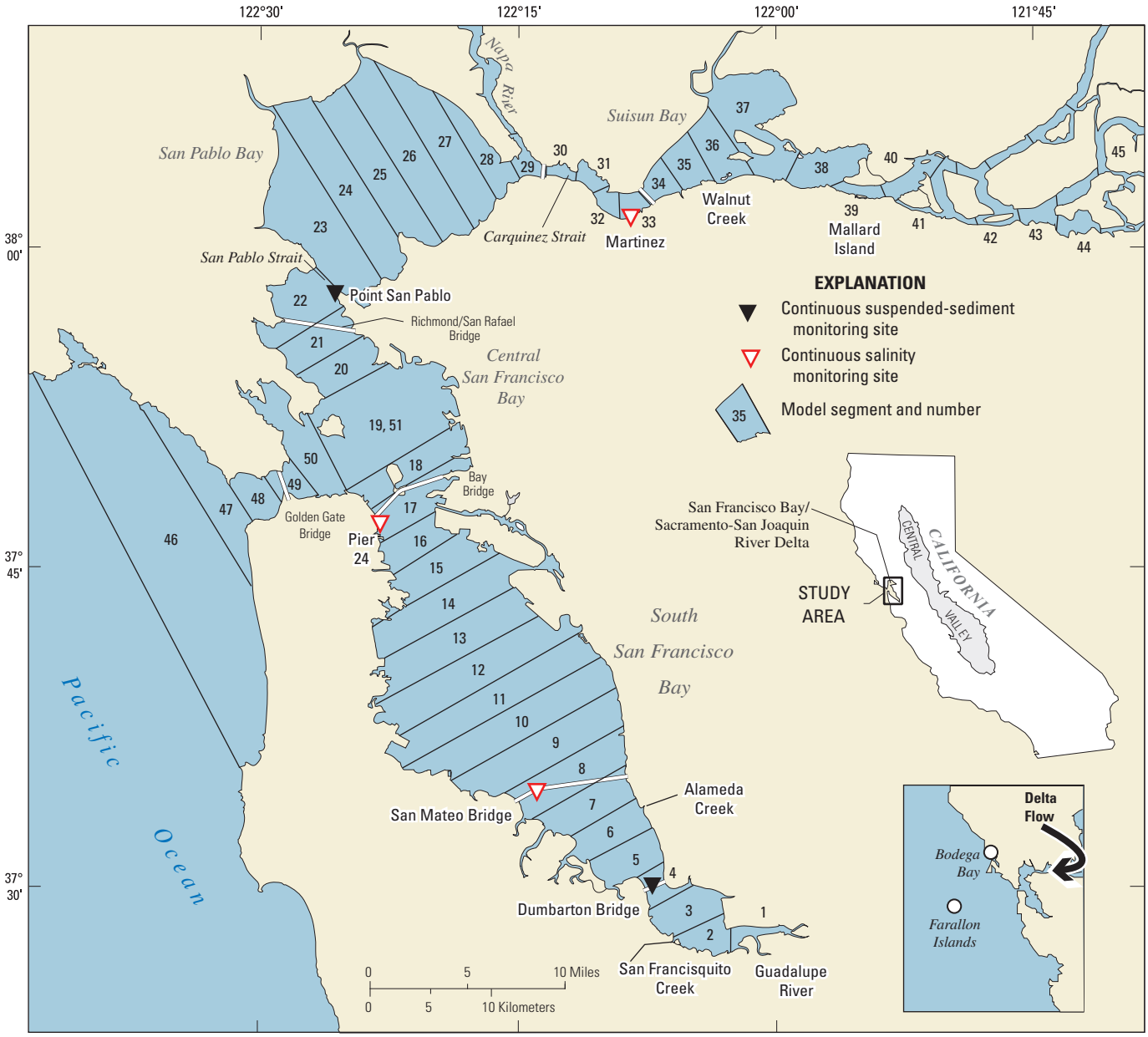

Figure 1. Uncles–Peterson salinity model segmentation of San Francisco Bay, California, and locations of U.S. Geological Survey continuous salinity monitoring sites (modified from Uncles and Peterson, 1996).

Description of the Study Area

San Francisco Bay is made up of multiple broad, shallow bays connected by deep, narrow channels. The seaward boundary of the Bay is the Golden Gate and the landward boundary is Mallard Island in the north and the Guadalupe River in the south (*fig. 1*). The average depth in the Bay is less than 6 m with depths as great as 100 m at the Golden Gate Bridge (Conomos, 1979). The Bay receives 90 percent of its mean annual freshwater inflow from the Sacramento–San Joaquin River Delta (Delta), which drains 40 percent of California including the agriculturally rich Central Valley. The remaining 10 percent of freshwater inflow comes from local tributaries and waste-water treatment plant effluent. North San Francisco Bay is a partially mixed estuary with estuarine circulation maintained by the density difference between freshwater river inflow from the Delta and Pacific Ocean seawater (Conomos and Peterson, 1977). South San Francisco Bay is typically well-mixed because of small freshwater inflows.

In San Francisco Bay, an annual cycle of sediment deposition and resuspension begins with a large influx of sediment during large freshwater flows in winter (Conomos and Peterson, 1977; Goodwin and Denton, 1991; McKee and others, 2006). The first freshwater pulse in winter delivers a relatively large amount of sediment, compared to subsequent pulses (Goodwin and Denton, 1991). For example, data from Ruhl and Schoellhamer (2004) show that the first pulse in winter 1997 was about a factor of four greater than the second pulse. Typically, discharge from the Delta contains over 60 percent of the fluvial sediments that enter the Bay (McKee and others, 2006), though this percentage varies from year to year. Much of this new sediment deposits in shallow water subembayments, especially in north San Francisco Bay seaward from the Delta (Krone, 1979; and Ruhl and Schoellhamer, 2004). A stronger sea breeze during spring and summer causes wind-wave resuspension of bottom sediment in these shallow waters and increases SSC (Schoellhamer, 1996, 2002; Ruhl and others, 2001; Ruhl and Schoellhamer, 2004; and Warner and others, 2004). The ability of wind to increase SSC is greatest early in the spring, when unconsolidated fine sediments can be resuspended easily. As the fine sediments are winnowed from the bed, however, the remaining sediments progressively become less erodible (Krone, 1979; and Nichols and Thompson, 1985). The result is that tidally averaged SSC is greatest in spring, decreases during summer, and is least in fall (Schoellhamer, 1996, 2002; and Ruhl and Schoellhamer, 2004).

Uncles–Peterson Salinity Model

The Uncles–Peterson salinity model (Uncles and Peterson, 1995, 1996) uses a box-model approach wherein each segment is assumed to be well mixed. The Bay is represented by 50 width-averaged segments (*fig. 1*), each composed of two layers (*fig. 2*). Salinity is assumed to be well-mixed (homogeneous) across the width of each layer. Segments 19 and 51 refer to the same segment connecting the three major subembayments. This redundancy is needed for numerical purposes. The upper layer of each segment represents the shallows (0 to 5-m depth) and the lower layer represents the channel (greater than 5-m depth). Tidally averaged residual currents advect water and theoretical mixing rates constrain the dispersive exchanges of water between segments. A tidally averaged salinity field is solved implicitly using a 1-day time step to enable the model to run over a decadal time scale in a relatively short period of time. The model has been calibrated previously to salinity (Knowles, 1996).

The width-averaged governing equation describing the salinity (S) balance is given by

$$\frac{\partial}{\partial t}(BS) = -\frac{\partial}{\partial x}(BUS) - \frac{\partial}{\partial z}(BWS) + \frac{\partial}{\partial x}\left(BD\frac{\partial S}{\partial x}\right) + \frac{\partial}{\partial z}\left(BK\frac{\partial S}{\partial z}\right) \quad (1)$$

where

B is average segment width, in m;

S is salinity, unitless;

U is laterally and tidally averaged longitudinal residual current velocity, in meters per second (m/s);

W is laterally and tidally averaged vertical residual current velocity, in m/s;

D is longitudinal dispersion coefficient, in square meters per second m^2/s; and

K is eddy diffusivity, in m^2/s.

The variables x and z represent the longitudinal along-estuary direction and vertical direction, respectively. Equation 1 is solved implicitly for the residual (tidally averaged) salinity field by LU decomposition by using a 1-day time step. The residual current field is calculated algebraically.

Input data used in the mass-balance calculations include daily root-mean-square coastal sea level elevation at the Golden Gate Bridge in San Francisco to represent tides, near-bed coastal salinity, precipitation, evaporation, and Bay inflow from the Delta and local tributaries. The dynamics of coastal sea-level elevation as a function of the tides is well known and is predicted accurately. The near-bed coastal salinity boundary condition is taken as salinity measured at the Farallon Islands, 35 kilometers (km) off the coast from the Golden Gate Bridge. Precipitation and evaporation are variable throughout the Bay, although their effects on salinity are minimal. One daily value of each is assumed to apply to all model segments. Delta outflow is the most critical of all model inputs and is calculated by DAYFLOW (California Department of Water Resources, 1986), which the Uncles–Peterson model uses directly. DAYFLOW errors are thought to be relatively small (less than 10 percent) on a monthly time-scale, except for extreme low, or perhaps, high flows (Uncles and Peterson, 1996). Inflow from local tributaries is assumed to be a fraction of Delta outflow determined from historical data.

Salinity boundary conditions exist at the Pacific Ocean (box 46) and the Delta (box 45), and a zero-flux boundary condition is applied at the most southern point of South San Francisco Bay (box 1) to ensure conservation of mass. The lower segment salinity at box 46 is set to the coastal salinity, while the upper segment salinity remains variable since it is affected more by buoyant freshwater inputs from upstream sources. Delta outflow entering the Bay is freshwater; therefore, salinity is set to zero in both layers of box 45. Additionally, local tributary inflow salinities are set to zero.

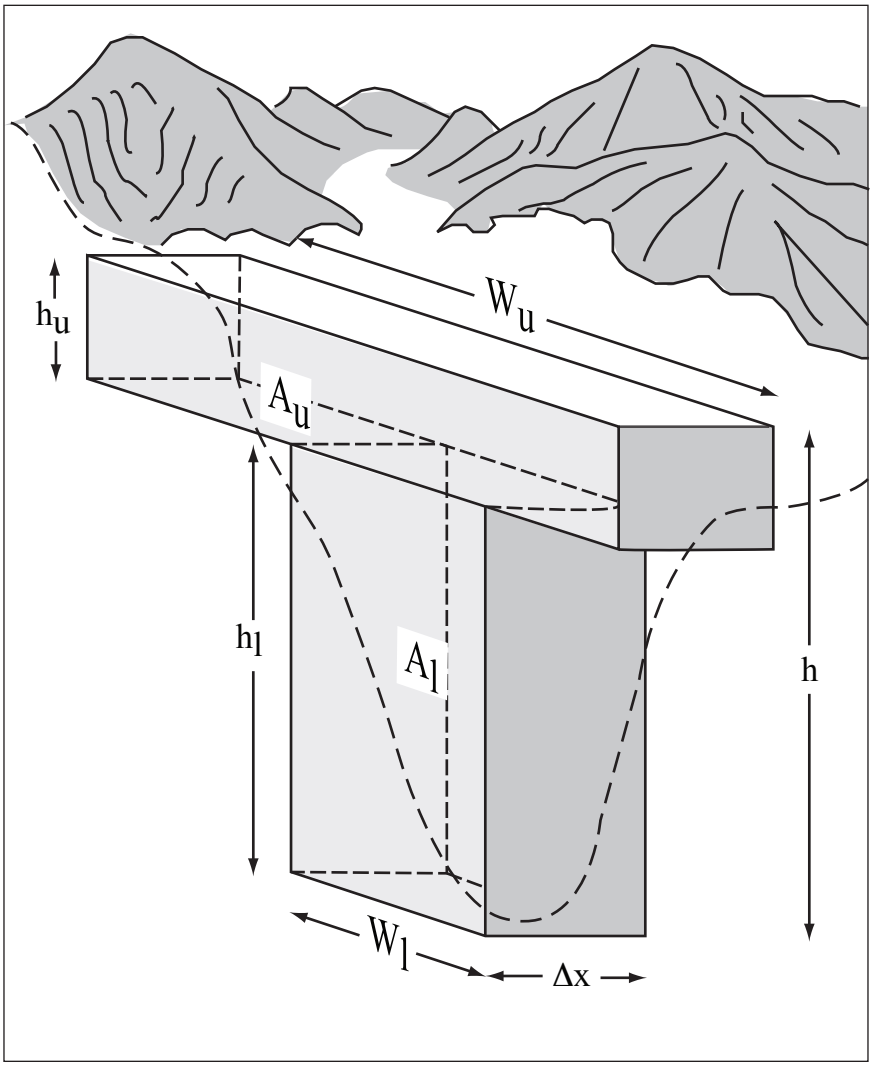

Figure 2. Sample model segment composed of an upper and lower layer (Uncles and Peterson, 1996).

Mixing Processes

Longitudinal mixing within the estuary occurs through advective and diffusive processes. The Uncles–Peterson model accesses prescribed maximum tidal currents tabulated for each segment as a function of root-mean-square sea-level elevation from a high resolution, depth-averaged intra-tidal model of the Bay (Uncles, 1991). Estuary-surface slope, residual velocities and flows are calculated using Officer's (1976) analysis of gravitational circulation. Separate longitudinal density gradients are calculated in the surface and bottom layers with the total shear force of the upper layer transferred to the lower layer. Depth- and tidally averaged current speed, $\overline{U}$ is approximated by

$$\overline{U} = \int_0^{2\pi/t} \left| U_{tid} \cos \omega t + U_{res} \right| dt \qquad (2)$$

where

U_{tid} is maximum tidal current speed, in meters per second (m/s) ;

U_{res} is depth- averaged residual current velocity, in m/s ; and

ω is semidiurnal tidal frequency, in second^{-1} .

Longitudinal diffusion is described as a combination of longitudinal dispersion due to tidal trapping (Okubo, 1973, as described in Fischer and others, 1979) and an additional 10 square meters per second (m^2/s) to account for transverse flows and wind effects

$$D = \frac{D'}{1+r} + \frac{r\bar{U}^2}{2k(1+r)^2(1+r+\omega/k)} + 10 \quad (3)$$

where

D is longitudinal dispersion, in m^2/s;

D' is longitudinal diffusivity in the main channel, in m^2/s;

r is ratio of trap volume to channel volume, dimensionless; and

k^{-1} is characteristic exchange time between traps and the channel, in seconds.

When $Z = 1.4 \times 10^{-4} s^{-1}$, $r = 0.1$, and $k{-}1 = 10^4$ s are used to represent San Francisco Bay, equation 3 simplifies to

$$D = 1000\bar{U}^2 + 10. \quad (4)$$

This approximation of the longitudinal diffusion is accompanied by an adjustable calibration factor. Previous efforts (Knowles, 1996) to define calibration factors improved model results compared to uncalibrated results described by Uncles and Peterson (1995, 1996).

Vertical mixing between the upper and lower segment layers is sensitive to density stratification. The Richardson number, R_i, which measures the stability of stratification, is calculated as

$$R_i = \frac{g(\partial\rho/\partial z)}{\rho\left|\partial u/\partial z\right|^2} \quad (5)$$

where

$\partial\rho/\partial z = (\rho_l - \rho_u)/H$

ρ_l is density in the lower layer, in kilograms per cubic meters (kg/m^3);

ρ_u is density in the upper layer, in kg/m^3;

H is total height of the segment, in m; and

$\partial u/\partial z = \bar{U}/H$.

The Richardson number is constrained to $0 < R_i < 2$ so that vertical mixing does not become too small. The Uncles and Joint (1983) expression is used to approximate the vertical eddy viscosity, υ',

$$\upsilon' = 2.3\times10^{-3} H^2 \left|\partial u/\partial z\right|. \quad (6)$$

The vertical eddy viscosity is used to calculate both the eddy diffusivity and the eddy viscosity, as described by Munk and Anderson (1948). The eddy diffusivity is calculated as

$$K = \upsilon'(1+1.33R_i)^{-3/2} \quad (7)$$

and the eddy viscosity is calculated as

$$\upsilon = \upsilon'(1+10R_i)^{-1/2}. \quad (8)$$

Once again, an adjustable calibration factor is applied to the eddy diffusivity for improved model results.

Salinity Model Validation

The Uncles–Peterson salinity model was validated by comparing simulated salinity with continuous salinity data collected in water year 1999 (October 2008–September 2009; Buchanan, 2000). Upper and lower sensor data at each site were compared with simulated salinity from the upper and lower layers of the corresponding model segments. This water year has not been used for previous model calibration and, therefore, was used to validate the model. After less than 1 month of model spin-up time, the model became insensitive to the initially prescribed salinity field. Results from the Martinez, Pier 24, and San Mateo Bridge sites (*fig. 1*) are shown in *figures 3–5*, representing North Bay, Central Bay, and South Bay. Model simulations under-predicted salinity in North Bay and slightly over-predicted salinity in Central and South Bays. Overall, the model was able to reasonably predict the salinity field throughout the Bay, indicating that mixing and transport are well defined.

Results of the salinity validation runs demonstrate that the model reasonably represents longitudinal and vertical mixing on an inter-tidal time scale by successfully simulating the Bay-wide salinity field.

Applications of the Uncles–Peterson Salinity Model

Past studies have described the hydrologic effects of climate change on the San Francisco Bay drainage basin. They include reduced snowpack storage, higher flood peaks during the rainy season, and reduced warm-season flows after April (Gleick, 1987; Roos, 1989; Lettenmaier and Gan, 1990; Jeton and others, 1996; Gleick and Chalecki, 1999; Knowles and Cayan, 2002; Snyder and others, 2002; Dettinger and others, 2004; and Knowles and Cayan, 2004). Knowles and Cayan (2004) used the Uncles–Peterson salinity model in conjunction with the Bay–Delta watershed model (BDWM) (Knowles, 2000) to simulate the effects on Bay salinity as a result of altered freshwater flows. Results showed that altered freshwater flows would increase salinity and potentially adversely affect freshwater supplies drawn from the Delta. Uncles

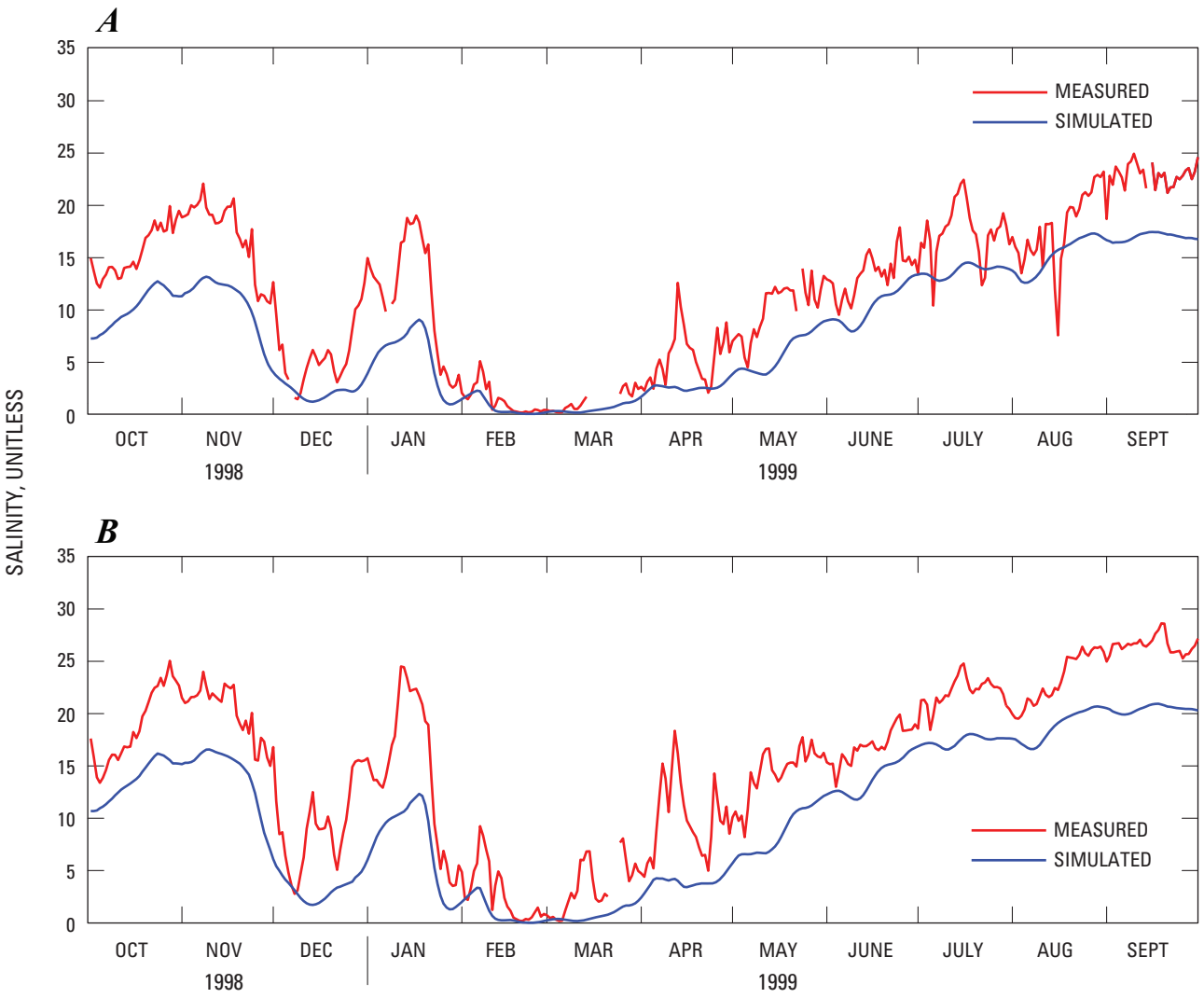

Figure 3. Time series of salinity model validation of (*A*) near-surface and (*B*) near-bottom at Martinez, North San Francisco Bay, California, water year 1999.

(2003) showed that sea-level rise also would increase salinity by simulating salinity while incrementally increasing the depths of the upper segments in the UP salinity model.

Sediment-Transport Model

A sediment-transport model was incorporated into the existing UP salinity model to simulate sediment transport in San Francisco Bay on a decadal time scale (Lionberger, 2003). A daily time step is used to compute tidally averaged SSC and net sedimentation. Mixing and advection rates calculated by the salinity model are used to exchange sediment between models segments. Exchange of bed sediments and suspended sediments is calculated with a simplified bed algorithm.

Input Data

Daily suspended-sediment flux from the Delta to the Bay at Mallard Island is estimated for water years 1995–2003 by McKee and others (2006). These data were used to develop a relation (rating curve) for the suspended-sediment flux at Mallard Island as a function of Delta outflow and lagged suspended-sediment concentration in the Sacramento River at Freeport (80 km upstream of Mallard Island). SSC data are available at Freeport since 1979. For the period 1957–79, SSC data at the I Street Bridge in Sacramento were used, which virtually are the same data as at Freeport (Wright and Schoellhamer, 2004). Prior to 1957, only discharge data are available on the Sacramento River, so a relation between discharge and SSC was used to estimate SSC. A 3-day lag for SSC at Freeport to simulate travel time through the Delta produced the best fit. The rating curve is

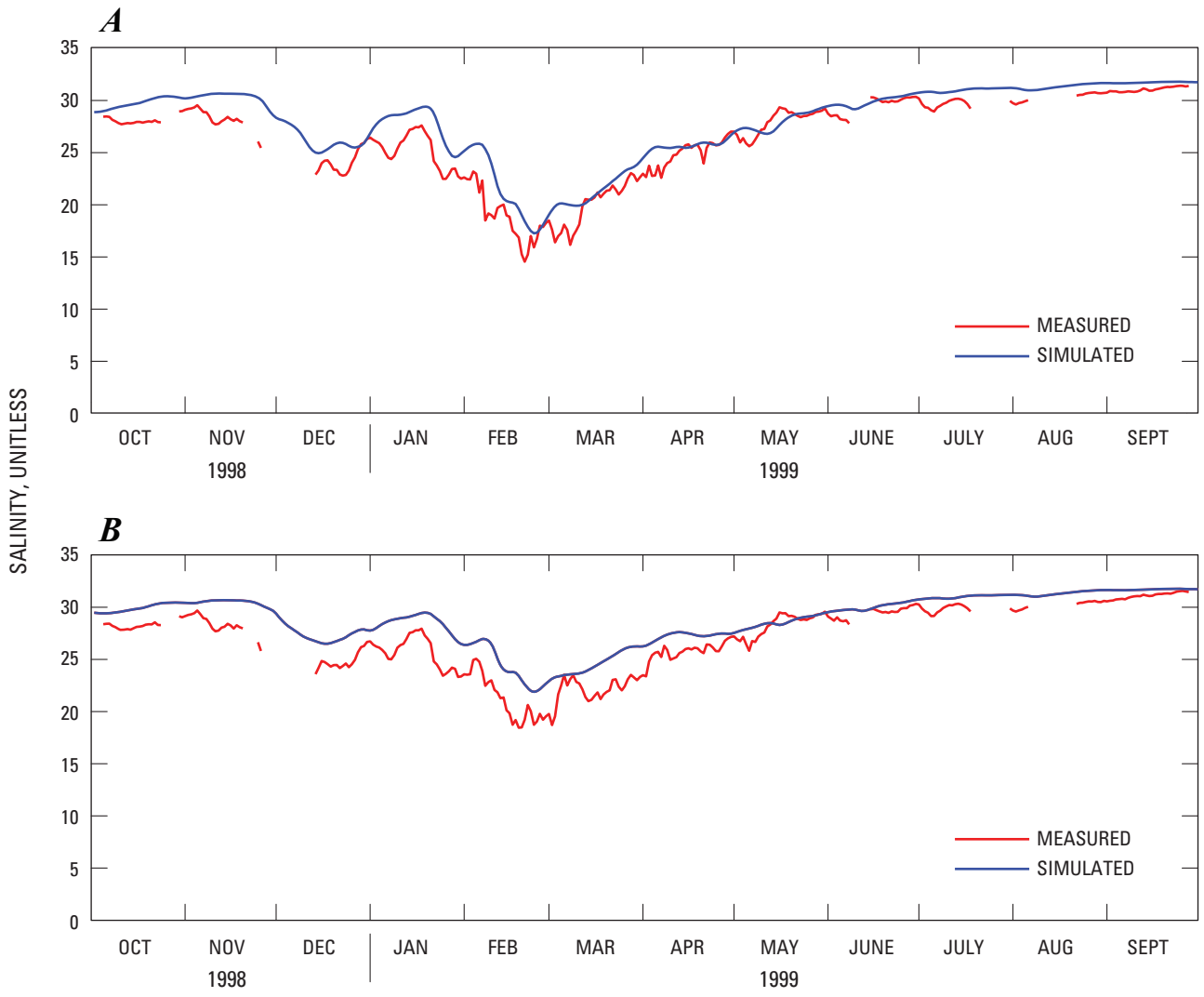

Figure 4. Time series of salinity model validation of (*A*) near-surface and (*B*) near-bottom at Pier 24, Central San Francisco Bay, California, water year 1999.

$$F_{mal} = 0.00079 \cdot Q^{1.74} C_{fre}^{0.52} \quad (9)$$

where

F_{mal} is suspended – sediment flux, in metric tons per day (t/d);

Q is Delta outflow, in cubic meters per second (m^3/s) (California Department of Water Resources, 1986); and

C_{fre} is daily mean suspended – sediment concentration in the Sacramento River at Freeport, in milligrams per liter (mg/L).

Figure 6 shows that equation 9 reproduces the sediment flux data fairly well and the squared correlation coefficient is 0.89.

Including C_{fre} enables the rating curve to simulate the decrease in sediment load, in time, as a result of diminishment of pulse of sediment from hydraulic mining and increased damming of upstream tributaries (Wright and Schoellhamer, 2004). Freeport has the longest recorded sediment record closest to the upstream boundary condition of the model.

An assumption must be made about deposition in the 80 km of ungaged channel between Freeport and the Bay–Delta border at Mallard Island. Ogden Beeman and Associates and Ray B. Krone and Associates (Ogden Beeman and Associates and Ray B. Krone and Associates, 1992) developed a sediment budget for San Francisco Bay for 1956–1990 and assumed that all of the sediment supplied by Central Valley rivers passed through the Delta and into San Francisco Bay (that is, no deposition in the Delta). Wright and Schoellhamer (2005) used measurements to construct a sediment budget for the Delta for water years 1999–2002 that showed that about two-thirds of the suspended sediment that entered the Delta

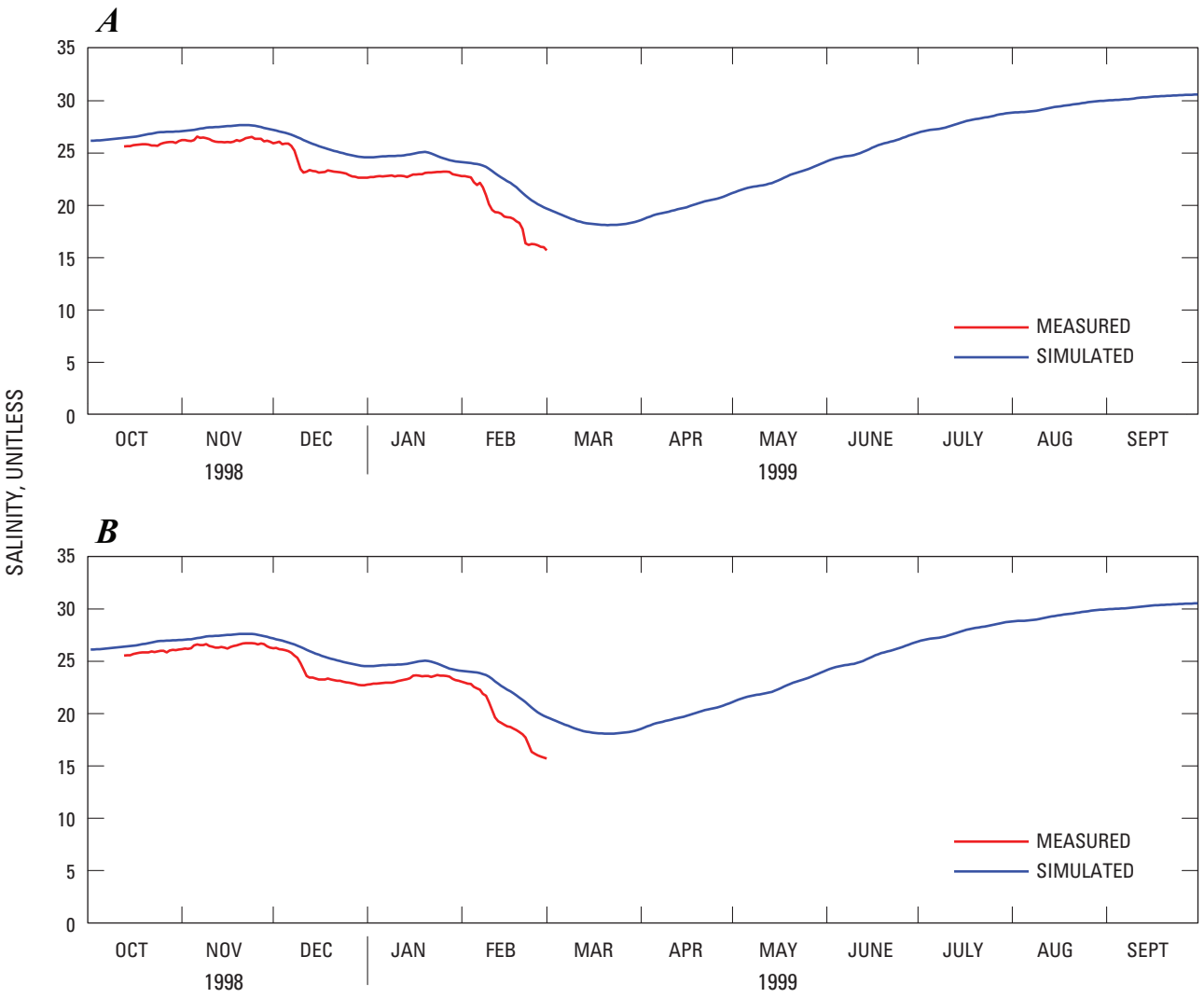

Figure 5. Time series of salinity model validation of (*A*) near-surface and (*B*) near-bottom at San Mateo Bridge, South San Francisco Bay, California, water year 1999. Sensors were removed in March for bridge repairs.

from the Central Valley was permanently deposited in the Delta and never reached San Francisco Bay. Because of this uncertainty, we assume that prior to water year 1991 one-half of the suspended sediment that entered the Delta was permanently deposited there. This value of one-half was chosen to be between zero (Ogden Beeman and Associates and Ray B. Krone and Associates, 1992) and two-thirds (Wright and Schoellhamer, 2005).

The mass of sediment supplied to the Bay from the Delta was added to box 38 for every daily time step. The model has boxes upstream and downstream that advect and disperse sediment, so adding mass as calculated by equation 9 to box 38 did not produce the desired flux boundary condition at Mallard Island. To match one-half of the sediment flux into the Delta estimated by Ogden Beeman and Associates and Ray B. Krone and Associates (1992) prior to water year 1991, F_{mal} was multiplied by a factor of 0.81. To match the sediment flux to the Bay estimated by McKee and others (2006) for water years 1995–2003, F_{mal} was multiplied by a factor of 1.09 beginning in water year 1991. The multipliers differ because the flux estimate techniques differ.

Wind data from two meteorological stations, San Francisco Airport in South Bay (National Climatic Data Center) and Suisun Bay (U.S. Geological Survey [USGS]), were chosen to represent the varying conditions between North Bay (boxes 21–38, 46–50) and South Bay (boxes 1–20). Bed shear resulting from wind wave orbitals in the water column is proportional to the square of the wind speed at the surface. Available hourly wind-speed data from each site were squared and then averaged over 24 hours to obtain a daily average, squared, wind speed. When hourly data were not available, the mean wind speed for that hour of the year from the period of record was used (*fig. 7*). Winds vary on an annual cycle, with stronger westerly winds in spring and summer, because temperature gradients between the coast and inland valleys are greatest, and weaker westerly winds in fall and winter (*fig. 7*).

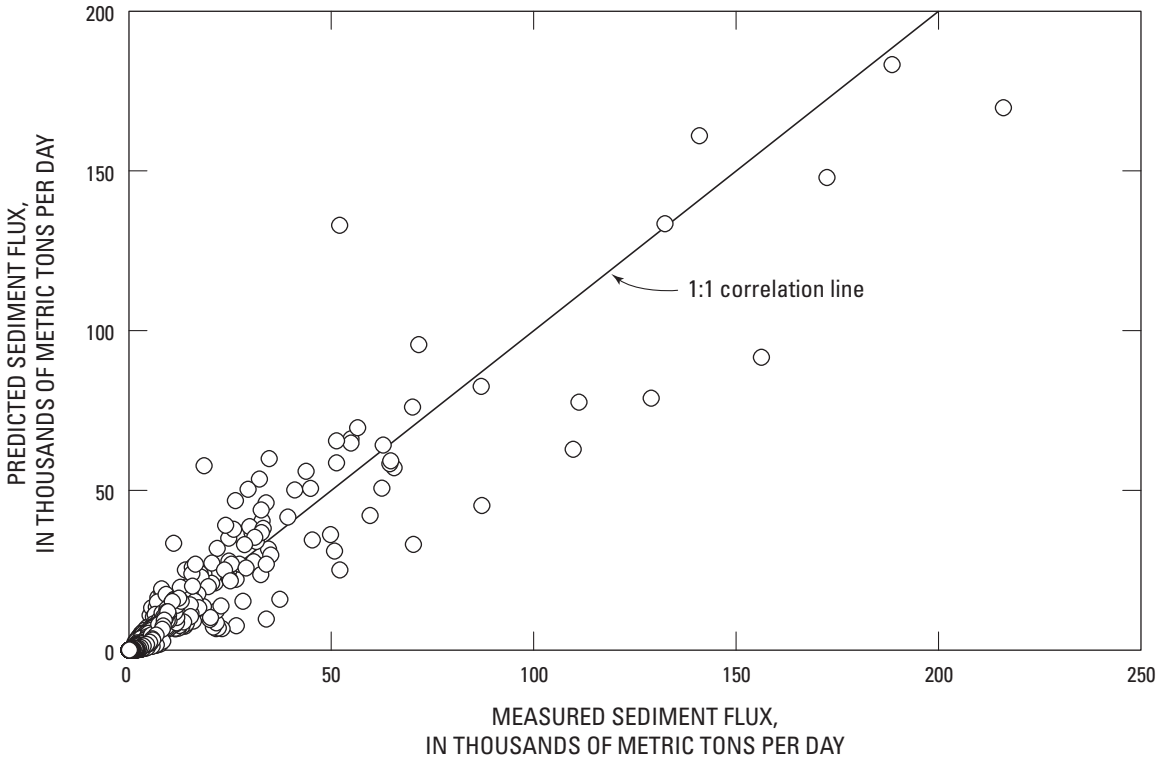

Figure 6. Comparison of suspended-sediment flux measured by McKee and others (2006) and predicted by equation 9. The line is the line of perfect agreement.

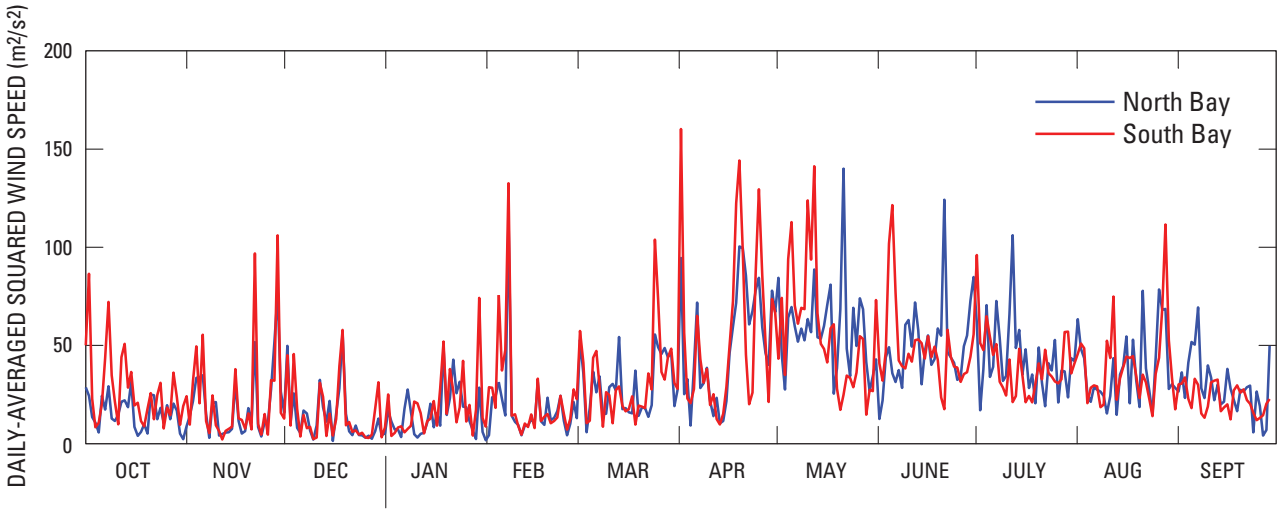

Figure 7. Daily mean squared wind speed for North Bay and South Bay used when hourly wind data are unavailable.

Table 1. Land subsidence rates in boxes 1-4 for 1934-60, 1960–67, and 1967-82.

	Subsidence rates (millimeters per year)		
	1934–60	1960–67	1967–82
Box 1	22.6	38.1	1.9
Box 2	16.9	28.6	1.4
Box 3	11.3	19.1	1.0
Box 4	5.6	9.5	0.5

Land-surface subsidence in Santa Clara Valley owing to overdraft of ground water in the first half of the 20th century affected sediment-bed elevations south of Dumbarton Bridge (boxes 1–4). Poland and Ireland (1988) detail land subsidence from 1934–60, 1960–67, and 1967–82, which peaked in the middle 1960s (*table 1*). Subsidence rates were used to adjust sediment bed elevations daily in the upper layer of boxes 1–4. Recovery of water levels since the middle 1960s has been substantial and has reduced or eliminated subsidence in the region, so zero net elevation change is assumed after 1982. Sediment-bed elevations in the upper layer of all segments also are adjusted daily to simulate sea-level rise, which is assumed to be 3 millimeters per year (mm/y). This value was selected because (1) global sea-level rise was 1.5–2.0 mm/y during the 20th century and 3.1 ± 0.7 mm/y from 1993 to 2003 (Bindoff and others, 2007) and (2) sea-level rise for San Francisco Bay during the 20th century was 2.17 mm/y (Flick and others, 2003). A sensitivity test (not shown) found that simulation results are not sensitive to this value.

Sediment loss to tidal marsh deposition is estimated. A wetland area of 163 square kilometers (km^2) from the Goals Project (1999) is multiplied by a rate of sea level rise of 2.17 mm/y for San Francisco Bay from 1900–99 (Flick and others, 2003). This assumes that the marsh accretes inorganic sediment at a rate to maintain its elevation, relative to sea level. Organic sedimentation is neglected which would lead to overestimation of inorganic sedimentation, This component of the Bay sediment budget, however, is relatively small so it does not significantly affect the overall results. Tidal marsh sedimentation is distributed between regions, relative to their total marsh area. The assumed sea-level rise rate for wetlands differs slightly from that for the open waters of the bay, but results were not sensitive to this value.

Suspended-Sediment Concentration Boundary Conditions

Sediment boundary conditions are specified at the Delta (box 38) and at the Pacific Ocean (box 46). Bay–Delta suspended-sediment flux (eq. 9) represents the Delta boundary condition and SSC in the lower layer of box 46 is held constant at 5.7 mg/L, the long-term mean concentration from monthly water-quality sampling by the USGS (*http://sfbay.wr.usgs.gov/access/wqdata*). The upper layer of box 46 is left free to vary, as it is affected more by buoyant freshwater inputs from upstream sources. Mass conservation in segment 1, the southern end of South Bay, is maintained by a no-flux boundary condition.

Daily tributary sediment load is simulated for Napa River, Walnut Creek, Alameda Creek, San Francisquito Creek, Guadalupe River, and multiple stream groups (Porterfield, 1980) as outlined in *table 2*. Sediment load for unmeasured stream groups are calculated as a function of a nearby creek, assuming conditions are similar. Sediment is added into the box nearest to the tributary entrance or distributed between boxes in a stream group region.

Suspended-Sediment Algorithm

The sediment-transport model was incorporated as a subroutine into the existing UP salinity model to simulate sediment transport on a decadal time scale (1940–2006). Daily-average suspended-sediment concentration (SSC) and daily net sedimentation are computed. Mixing and advection rates calculated by the salinity model are used to simulate suspended-sediment exchange between model segments. Exchange between bed sediments and suspended sediments is calculated explicitly with a simplified bed algorithm.

The sediment model requires more realistic water depths than the salinity model, especially in the upper layer, because wind-wave resuspension increases as water depth decreases. The salinity model assumes that depth in the upper layer is 5 m. This is an unrealistic depth for the sediment model since most shallow areas in the Bay are shallower than 5 m. On the USGS San Francisco Bay bathymetry website, zTool can be used to display a cross-section profile and compute volumes of user specified polygons (*http://sfbay.wr.usgs.gov/sediment/sfbay/zTool.html*). zTool was used to obtain lateral widths of the upper box layers. Lateral widths were multiplied by the longitudinal box widths to calculate planar areas of the upper layers. Upper layer volumes are divided by the planar areas to calculate width-averaged depths. On this basis, the Bay wide average upper layer depth was determined to be 3.7 m rather than the 5 m assumed for the salinity model. Depths are further adjusted by erosion of and deposition to the sediment bed. Geometry data used by the salinity model were left unchanged.

Table 2. Summary of tributary sediment loads (Porterfield, 1980) and Uncles–Peterson box distribution.

Box	Sediment source	Suspended load
2	Guadalupe River and stream group 9	3.38*Guadalupe
3	San Francisquito Creek	San Francisquito Creek
8	Alameda Creek	Alameda Creek
4-18	Remainder of stream group 10	1.97*San Francisquito Creek
12	Colma Creek	1.29*San Francisquito Creek
9-22	Part of stream group 7	0.21*Alameda Creek
23	Part of stream group 1	0.19*Napa
24	Petaluma River	0.17*Napa
25	Part of stream group 2	0.20*Napa
26	Sonoma Creek and other Sonoma drainage	0.39*Napa
29	Napa River gage and other Napa drainage	1.53*Napa
34	Walnut Creek and remaining contribution	1.50*Walnut Creek
31-41	Stream group 5 and remainder of stream group 6	0.90*Walnut Creek
20-22, 50	Part of stream group 1	1.39*San Francisquito Creek

The daily mass-balance sediment algorithm begins by adding tributary sediment load to and removing wetland deposits from specific boxes throughout the UP model grid. The tributary loads are mixed within the estuary by implicitly solving the advection-dispersion transport equation (eq. 10) using mixing parameters calculated by the salinity model.

$$\frac{\partial}{\partial t}(BC) = -\frac{\partial}{\partial x}(BUC) - \frac{\partial}{\partial z}(BWC) + \frac{\partial}{\partial x}\left(BD\frac{\partial C}{\partial x}\right) + \frac{\partial}{\partial z}\left(BK\frac{\partial C}{\partial z}\right), \quad (10)$$

Mass exchange with the sediment bed is calculated explicitly. The new SSC (C_n) is a function of the initial concentration and mass exchanges with the sediment bed at the end of each time step (n)

$$C_n = C_o + (R_E - R_D)\frac{\Delta t}{H} \quad (11)$$

where

C_n is SSC after erosion and deposition, in mg/L;
C_o is SSC before erosion and deposition, in mg/L;
B is segment width, in m;
H is segment height, in m;
R_E is rate of erosion, in grams per square meter per second (g/m^2/s);
R_D is rate of deposition, in g/m^2/s; and
Δt is timestep duration, in second (s).

The daily time step is subdivided (Δt) so that no more than 25 percent of the sediment in suspension is deposited at one time. This is needed for model stability when SSC is high.

The rate of erosion is calculated as a function of the tidally averaged bed shear ($\overline{\tau_b}$)

$$R_E = c_E F \overline{\tau_b} \quad (12)$$

where

R_E is tidally averaged erosion rate, in g/m^2/s;
c_E is erosion calibration constant;
$\underline{F}$ is bed erosion factor; and
$\overline{\tau_b}$ is tidally averaged bed shear, in Newton per square meter (N/m^2).

The erosion calibration constant is a calibration coefficient that varies between regions and a bed erosion factor is calculated by the sediment bed algorithm described in the next section. Tidally averaged bed shear is composed of tidally averaged current shear (term 1) and wind wave shear (term 2).

$$\overline{\tau_b} = \frac{\rho g \overline{u}^2}{C_z^2} + c_w \frac{1}{2}\rho f \frac{\overline{u_w^2}}{\cosh kh}, \quad (13)$$

(1) (2)

where

ρ is density, in kg/m^3;
g is gravitational acceleration, 9.8 square meters per second (m^2/s);
$\overline{u}$ is tidally averaged current speed, in meters per second (m/s);
C_z is Chezy coefficient, in m$^{1/2}$/s;
c_w is wind calibration constant;
$\underline{f}$ is friction factor, 0.1 (Kamphius, 1975);
u_w is daily average wind velocity, in m/s;
k is wave number, in m^{-1}; and
h is average water depth, in m.

The second term on the right hand side is neglected in the lower layer because wind wave orbitals dissipate before reaching the bottom. Friction factor *f* is assigned a typical value of 0.1 (Kamphius, 1975) in a term that is scaled by the wind calibration constant, so the exact value of *f* is unimportant. The wind calibration constant is needed as a scaling factor to balance the tidal bed shear and the wind wave shear terms, and does not vary between model segments or subembayments.

Uncles–Peterson model hydrodynamics calculate a mean longitudinal current speed (model variable utideu) in each box, while tidal currents in the Bay vary between channels and shallows with stronger currents in the channels (Conomos and Peterson, 1977). Lateral currents are smaller and neglected. To prevent underestimated bed shear in the channels and overestimated bed shear in the shallows, a method was developed to adjust the channel average velocity for the two layers. The ratio of Manning's equation (Sturm, 2001) for each box layer, divided by Manning's equation for the whole box, is multiplied by the mean current speed to calculate a discharge-weighted tidally averaged current speed. The tidally averaged current speed for the upper layer is

$$\bar{u} = utideu \cdot \left(\frac{A_s}{P_s}\right)^{2/3} \Big/ \left(\frac{A_t}{P_t}\right)^{2/3} \quad (14)$$

where

A_s is the area of the shallows, in square meters m^2;
P_s is the wetted perimeter of the shallows, in m;
A_t is the total area of the shallows and the channel, in m^2; and
P_t is the total wetted perimeter of the shallows and the channel, in m.

and for the lower layer is

$$\bar{u} = utideu \cdot \left(\frac{A_c}{P_c}\right)^{2/3} \Big/ \left(\frac{A_t}{P_t}\right)^{2/3} \quad (15)$$

where

A_c is the area of the channel, in m^2; and
P_c is the wetted perimeter of the channel, in m.

The rate of deposition is a function of the suspended-sediment concentration,

$$R_D = c_D C_o \quad (16)$$

where

R_D is tidally averaged deposition rate, in $g/m^2/s$; and
c_D is deposition calibration constant, in m/s.

The deposition calibration constant is equivalent to the settling velocity. The daily time step is subdivided so that no more than 25 percent of sediment in suspension is deposited at one time. This is needed for model stability when concentrations are high. If the rate of deposition exceeds the mass of sediment in suspension, an error message is produced that says 'error in sediment mass conservation' with the box number and layer where the error occurred. The model will make the deposition rate equal the sediment in suspension and then continue to run.

The model is calibrated by adjusting the calibration constants c_W, c_E, and c_D to scale the rates of erosion and deposition. The model can be calibrated to either net sedimentation or SSC.

Sediment-Bed Algorithm

The rate of erosion is affected by shear strength properties of the sediment bed, which vary with depth and time owing to consolidation (Krone, 1999). Detailed data on the shear strength properties of the sediment bed in San Francisco Bay, however, are not available. Thus, a simplified method was developed to simulate the effect of consolidation by reducing the erosion potential of bed sediment as a function of depth and time since deposition. A bed algorithm was developed incorporating two layers, a top layer composed of freshly deposited, easily erodible sediment and a lower layer composed of partially consolidated to fully consolidated sediments. The top layer is composed of sediment deposited during the present or previous time steps for which the bed erosion factor (F) =1. The lower layer contains partially to fully consolidated sediment. The bed erosion factor of the lower layer was modeled based on a summary of sediment bed studies by Hayter (1984), who found that the erodibility of consolidated sediments varied in the top 4 centimeters (cm) of the bed but essentially was uniform below 4 cm where the critical shear stress for erosion roughly was four times greater than at the bed surface. The erosion rate calculated by the model is multiplied by the bed erosion factor (eq. 12), whose value depends on the sediment layer and the elevation of the sediment bed surface, relative to a vertical datum. The bed erosion factor varies from 1.0 to 0.25 and is given as

$$F = \begin{cases} 1.0 & z > 0 \\ 1.0e^{34.7z} & 0 \geq z > -0.04\,\text{m} \\ 0.25 & -0.04\,\text{m} \geq z \geq -\infty \end{cases} \quad (17)$$

where

z is the sediment-bed-surface elevation referenced to the bed datum.

Consolidation rate decreases exponentially with time and, assuming a constant deposition rate, F would decrease exponentially with depth, as shown in equation 17. The datum, $z = 0$, initially is set at the bed-surface elevation on day 1 of the simulation. If the top of the lower layer becomes higher than the datum elevation, the datum is reset to the current bed-surface elevation. Sediment remaining in the top layer after one full time step is incorporated into the lower layer and assumes the F value at that elevation, relative to bed datum. Sediment is eroded preferentially from the top layer before sediment is eroded from the lower layer.

Model Calibration

The sediment-transport model was calibrated to SSC by adjusting model coefficients for erosion (c_E, eq. 12), wind (c_W, eq. 13), and deposition (c_D, eq. 16) until simulated SSC most closely matched daily averaged, continuously measured SSC during water year 1999 at two locations in the Bay: Point San Pablo in North Bay and Dumbarton Bridge in South Bay (Buchanan and Ruhl, 2001). Water year 1999 is classified as having an average annual Sacramento–San Joaquin River basin outflow. The coefficient, c_E, was allowed to vary between subembayments, while the coefficients, c_W and c_D, were adjusted to a single bay-wide value. Values of the calibration coefficients are given in *appendix A*. Results of the calibration at Point San Pablo (*fig. 8*) and Dumbarton Bridge (*fig. 9*) show that a tidally averaged sediment-transport model can be used to predict the general trends in SSC associated with tidal fluctuations, residual velocity, and wind stress, although the spring-neap tidal SSC variability is underestimated. Validation of the model calibrated to SSC is given by Lionberger (2003). While calibrating to SSC, bathymetric change was unconstrained.

Data from bathymetric surveys have been used to estimate net change in sediment volume stored on the bottom of Suisun Bay (Cappiella and others, 1999), San Pablo Bay (Jaffe and others, 1998), and South Bay (Foxgrover and others, 2004) for periods ranging from 28 to 49 years (*table 3*). Sediment storage values were adjusted to remove subsidence and dredging. Analysis of survey data for Central Bay has yet to be completed. Prior to these USGS studies, Ogden Beeman and Associates and Ray B. Krone and Associates (1992) estimated bathymetric change in the subembayments, including Central Bay. These older estimates were done using the same surveys but in less detail than the USGS estimates and Lionberger (2003) found large discrepancies. Thus, we consider bathymetric change in Central Bay to be unknown. Regional sediment density data from sediment cores (Caffrey, 1995; Sternberg and others, 1986; and Bruce Jaffe, USGS, written commun., 2004) were used to convert net volumetric change to net mass change in order to compare estimated bathymetric change to simulated net sedimentation (*table 3*).

Net change in sediment storage calculated by the sediment-transport model, left unconstrained during the calibration to SSC, was compared with estimated values from Suisun Bay, San Pablo Bay, and South Bay. Results indicate that the model calibrated to SSC is not able to hindcast net sedimentation accurately (*table 3*). Simulated deposition in Suisun Bay and South Bay was too large and simulated erosion in San Pablo Bay was too large. Small errors in boundary conditions, hydrodynamic forcing, and cohesive sediment transport parameters can lead to erroneous simulated sedimentation (Schoellhamer and others, 2008).

The model was calibrated separately to net sedimentation, leaving SSC free to vary. The calibration coefficient c_D is equivalent to the settling velocity. McDonald and Cheng (1997) calibrated a sediment-transport model of San Francisco Bay to settling velocity and they found settling velocity was 1×10^{-3} m/s. This value was used to reduce the number of calibration coefficients. Additionally, the calibration coefficient, c_W, was reduced by a factor of 10 and left constant. The calibration coefficient, c_e, was adjusted within each subembayment until simulated net sedimentation equaled measured net sedimentation simultaneously in Suisun Bay, San Pablo Bay, and South Bay (*table 3*). Central Bay net sedimentation was assumed to equal zero. Values of the calibration coefficients are given in *appendix A*. Generally, upper layers were erosional and lower layers were depositional, as shown in *figure 10*. The box model approach assumes that eroded sediment in each layer instantly mixes throughout the layer. Consequently, lateral mixing in the upper layer and vertical settling from the upper to the lower layers is overestimated. Therefore, even though the model can be calibrated to net sedimentation in a region, it does not realistically simulate the distribution of erosion and deposition between the shallows and the channel.

Model Validation

Determining the effectiveness of the model calibrated to long-term net sedimentation requires comparison to a sedimentation data set not used for calibration. An alternative is to compare SSC results from the model calibrated to sedimentation to measured SSC, which sometimes is reasonable and sometimes is not (not shown). Even if validation to SSC was good, however, it does not demonstrate how effective the model is for simulating decadal time scale sedimentation. Sedimentation data for validation currently are available for a portion of South Bay roughly equal to boxes 1–10 from

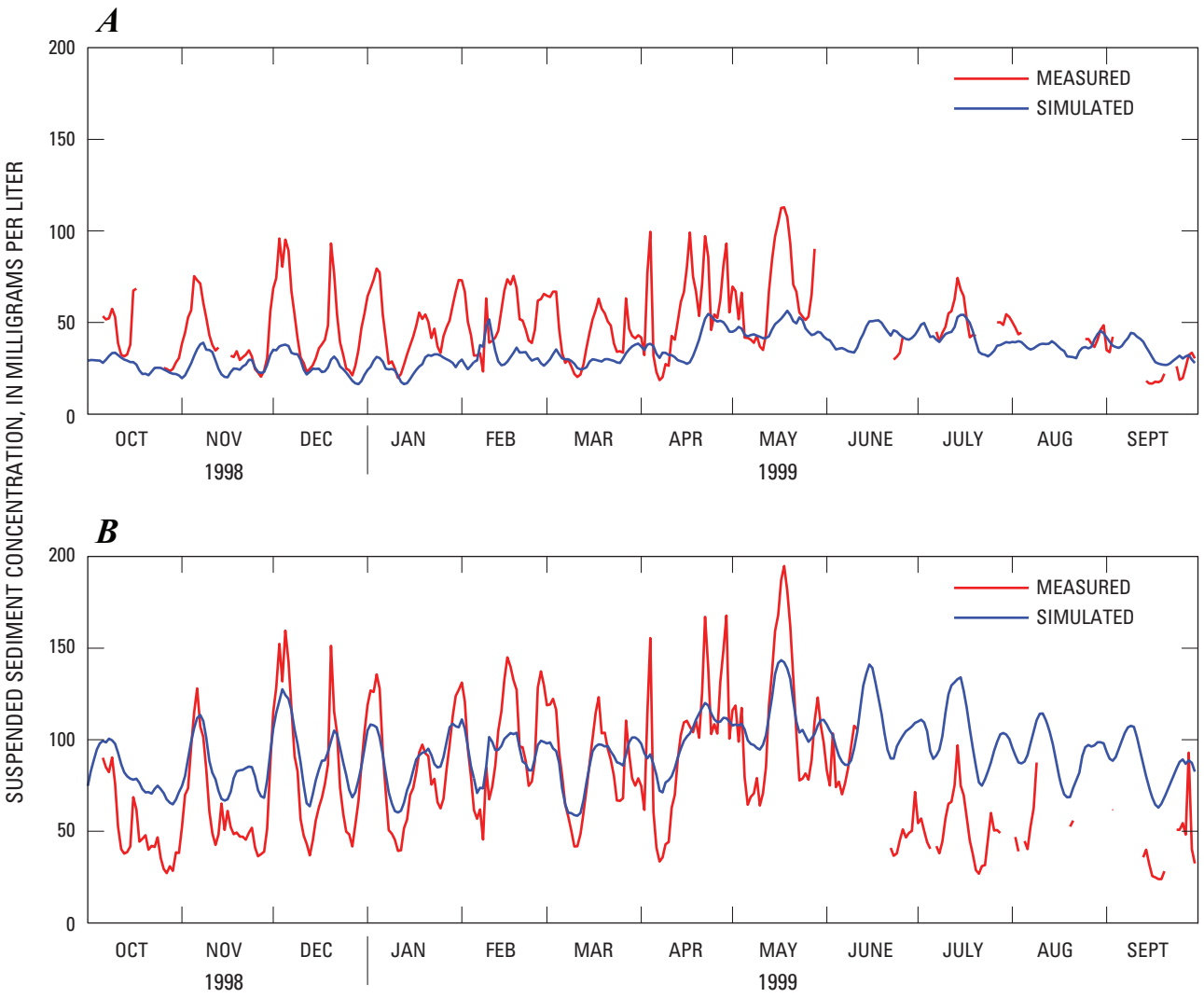

Figure 8. Time series of (*A*) mid-depth and (*B*) near-bottom measured (red) and simulated (blue) suspended-sediment concentrations at Point San Pablo, San Pablo Bay, California, water year 1999. Simulated values were calibrated to measured values.

1983–2005 (Foxgrover and others, 2007). Validation data for San Pablo Bay and Suisun Bay are unavailable, pending new bathymetric surveys and analyses to determine recent net bathymetric change.

The simulation period began on January 1, 1940, and the validation period began on October 1, 1983, and ended April 5, 2005, to approximate the period between bathymetric surveys (Foxgrover and others, 2007). No coefficients were adjusted. The measured and simulated net change in sediment mass in boxes 1–10 are in poor agreement (*table 4*). The simulation recreates the general pattern of deposition in the landward end of South Bay transitioning to erosion in the seaward direction, but the simulation underestimates observed deposition.

Poor quantification of sediment supply or biological changes not considered in the model may explain these poor validation results. We used Porterfield (1980) to estimate sediment supply, which is the most comprehensive study available but uses field data collected during the late 1950s. No sediment-supply data are available on any South Bay tributaries from 1973–2000, during which time South Bay watersheds urbanized. Schoellhamer and others (2006) found that sediment yield from the Guadalupe River decreased by a factor of 4 to 8 between the periods 1958–62 and 2003–05. Tides and wind are fairly constant year to year, so if decreased sediment supply is applicable to all of South Bay, the observed increase in deposition 1983–2005 (Foxgrover and others, 2007) cannot be explained by tides, wind, and sediment supply, the primary physical factors affecting sedimentation. At least two invasive species that have colonized the Bay since the 1980s may have altered deposition and erosion that the model fails to consider.

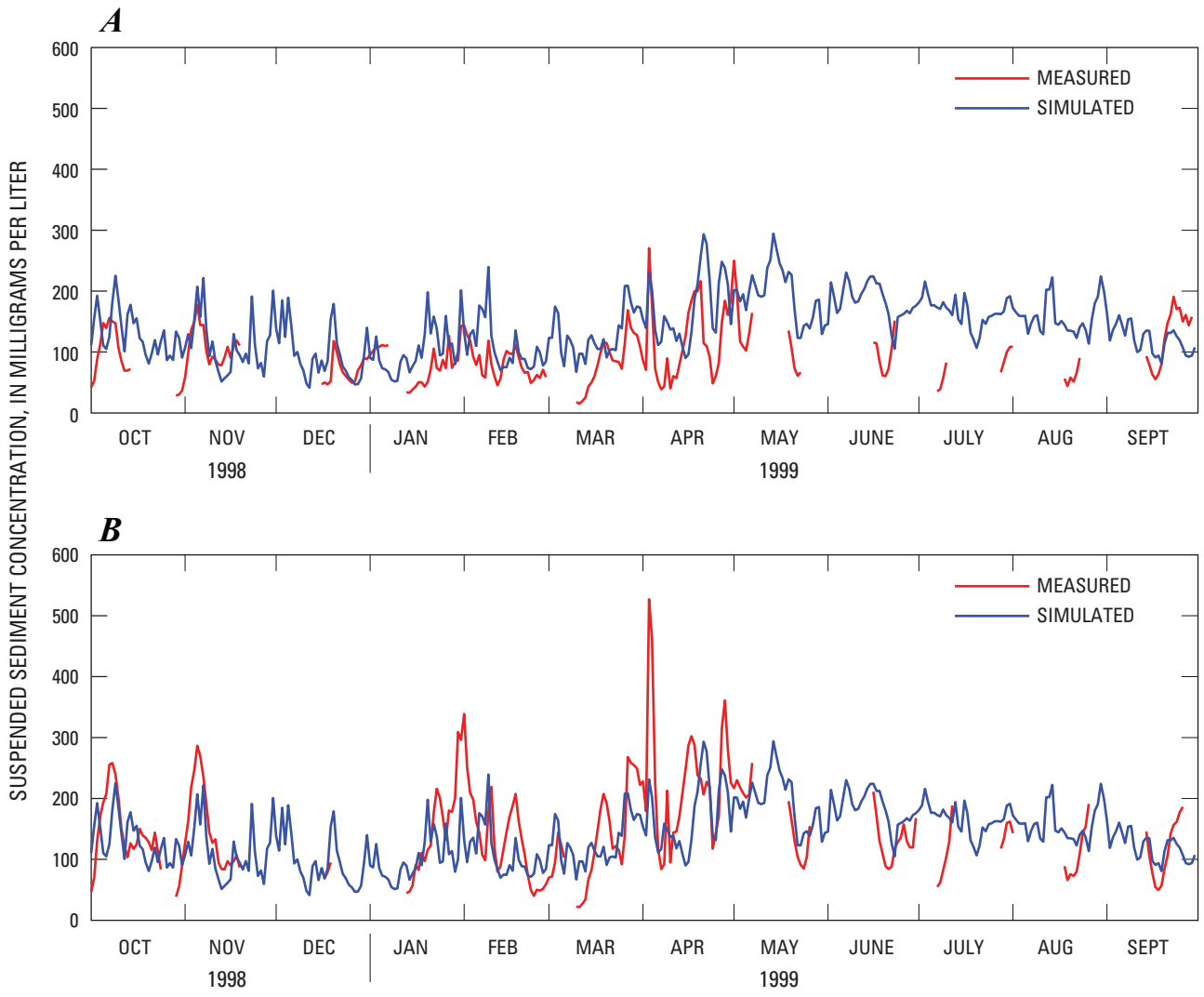

Figure 9. Time series of (*A*) mid-depth and (*B*) near-bottom measured (red) and simulated (blue) suspended-sediment concentrations at Dumbarton Bridge, South San Francisco Bay, California, water year 1999. Simulated values were calibrated to measured values.

Table 3. Estimated net sedimentation change based on bathymetric survey analysis and net sedimentation calculated by the sediment-transport model calibrated to suspended-sediment concentrations.

[Abbreviations: USGS, U.S. Geological Survey; UP, Uncles-Peterson]

Embayment and survey period	UP boxes	Sediment bed density (kg/m^3)[1]	USGS bathymetric change estimates (10^6 metric tons)	UP net sedimentation (10^6 metric tons)
Suisun Bay (1942–90)	29–39	863	–29	22
San Pablo Bay (1951–83)	23–28	730	–9	–168
South Bay (1956–83)	1–4	582	7.6	48.5
	5–8	667	–5.4	–.7
	9–11	808	–23.6	–3.9
	12–14	845	–19.2	–0.5
Central Bay (1942–90)	15–22, 46–50	996	0	–158

[1]Data from Caffrey (1995), Sternberg and others (1986), and Bruce Jaffe (USGS, written commun., 2004).

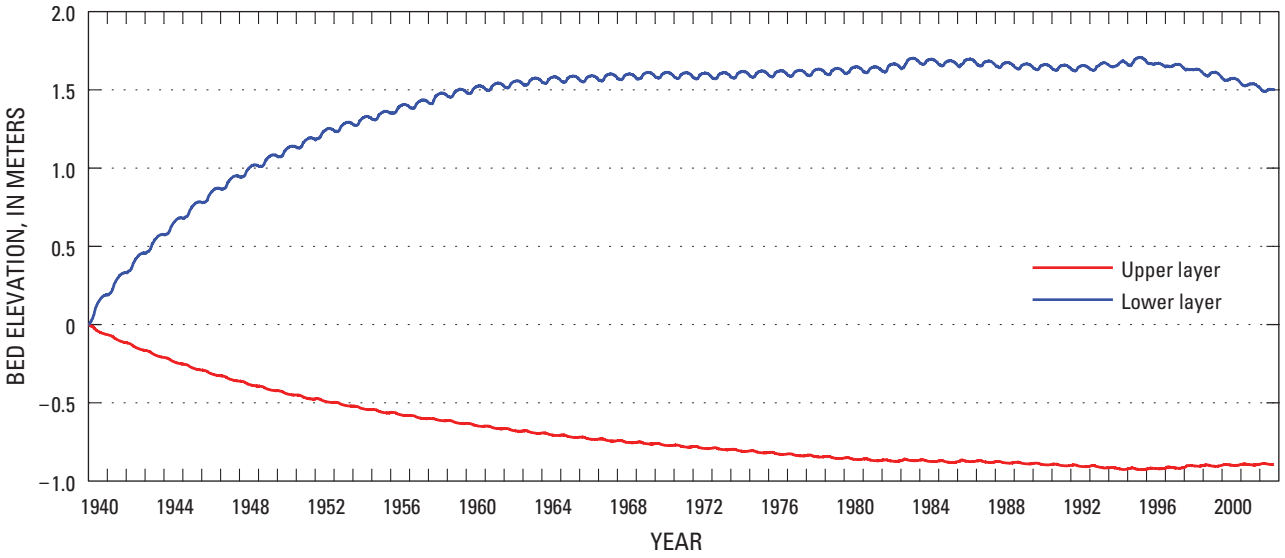

Figure 10. Time series of upper-layer (red) and lower-layer (blue) bed elevation change for box 5, for a simulation run from January 1, 1940, to September 30, 2002.

Mitten crabs invaded the estuary in 1992 and burrow into levees of tidal creeks, increasing sediment supply. Rudnick and others (2005) found that mitten crabs removed an average of 3 percent of tidal creek bank volume in South Bay over a 2-year study period. Slumping of banks was not included in their study. An estimate of the tidal creek length in boxes 1–4 is 24 km. Assuming a stream bank height of 1.5 m, burrowing depth of 0.5 m (Rudnick and others, 2005), and dry bulk densities from *table 3*, the sediment produced by mitten crabs over 14 years would be only about 4,400 megatonnes (Mt), three orders of magnitude less than the difference between measured and simulated volumetric change of 7,600,000 Mt in boxes 1–4. Thus, mitten crabs do not appear to explain the poor validation.

Corbula is a clam that displaced the previous benthic community in the late 1980s (Nichols and others, 1990) and has increased benthic filtering of the water column by a factor of up to several hundred (Thompson, 2005), removing much of the phytoplankton and zooplankton from the water column (Alpine and Cloern, 1992; Kimmerer and others, 1994). The clam has the potential to alter deposition and erosion coefficients. For example, in the Westerschelde Estuary in The Netherlands, about one-half of the sedimentation rate may be explained by biological processes, including bio-deposition by benthic filtering and changes in erodibility caused by changes in the benthic community (Widdows and others, 2004). Therefore, the deposition and erosion coefficients of the model are likely to vary with time, which, by necessity, a model validation cannot consider. Unfortunately, no data exist that can be used to estimate the effect of *Corbula* on sedimentation.

Sensitivity Analysis

Calibration coefficients, c_W (wind), c_E (erosion), and c_D (deposition) were each increased by 20 percent from the calibrated value to evaluate the sensitivity of simulated SSC and net sedimentation to variations in model parameters.

For the model calibrated to SSC, the upper and lower layers in each subembayment were grouped to evaluate the percent change in SSC compared to a 20 percent change in calibration coefficients (*table 5*). Positive values indicate an increase in SSC and negative values indicate a decrease in SSC. An increase in the deposition rate decreased SSC in the upper layers and increased SSC in the lower layers except Central Bay, where both upper and lower layer concentrations decreased. Both the erosion and wind coefficients caused SSC to increase in all layers and subembayments. All regions were moderately sensitive to changes to the deposition

Table 4. Validation of Uncles–Peterson sediment model calibrated to net sedimentation for South San Francisco Bay, California, 1983–2004.

Box	Net sedimentation, in 10^6 metric tons	
	Measured	Simulated
1	1.3	0.48
2	2.4	1.79
3	4.2	0.76
4	2.3	–0.46
5	1.5	–0.04
6	1.1	–0.30
7	–0.3	–0.89
8	–2.3	–1.29
9	–1.1	–3.37
10	–1.8	–5.40
Total	7.4	–8.72

rate. Increases in lower layer SSC resulted from more sediment depositing from the upper layer to the lower layer than deposited from the lower layer to the sediment bed, causing a net increase in SSC in the lower layer. South Bay was very sensitive to changes in the erosion rate because it has extensive shallow areas and relatively shallower lower layer depths, compared to other subembayments. The other regions had low sensitivity to increases in the erosion rate.

The sensitivity of the model calibrated to net change in sediment storage was quantified by the percent change in net sedimentation after increasing calibration coefficients 20 percent (*table 6*). Central Bay was not included since it was calibrated to zero net change. Positive values indicate an increase in bed mass and negative values indicate a decrease in bed mass. Suisun Bay was very sensitive to changes in both c_D and $c_{E;}$. San Pablo Bay was very sensitive to erosion rate increases c_E and c_W because of the large upper layer area representing the shallows. South Bay was moderately sensitive to changes in c_D and $c_{E.}$ Neither Suisun Bay nor South Bay net sedimentation was sensitive to changes in $c_{W.}$

User's Guide

The model and input files are available at *http://pubs.usgs.gov/sir/2009/5104/*. The UP model code is written in Fortran (file UPS.f). The sediment subroutine is named "sedsolve" and is called in the salsolve program. The salsolve program calls input files from a subfolder called inputs. Input files are text files with columns of numbers. The first number in the first line of file calib40.dat is the first day of the simulation with day 1 being January 1, 1940. The second number is the duration of the simulation, in days. To simulate from January 1, 1940, to September 30, 2006, the first number is 1 and the second number is 24,380. The third number is a multiplication factor (2.0) for flow from the Guadalupe River and Coyote Creek that was used to calibrate the salinity model and should not be modified. Subsequent lines in calib40.dat contain mixing calibration parameters that should not be modified. Other input files contain box geometry (bathymetZ.dat), maximum tidal currents tabulated for each box as a function of root-mean-square sea-level elevation (tidetabl.dat), daily salinity (sa4006.dat), daily evaporation (ev4006.dat), daily precipitation (pr4006.dat), daily tidal range (ti4006.dat), daily squared wind speed (win4006.dat), daily SSC at Freeport lagged by 3 days (fpt4006.dat), daily sediment mass lost to wetlands (wet4006.dat), daily tributary sediment load (trib4006.dat), daily flowrate from the Delta (f4006.dat), and an initial salinity and residual velocity for each box (init40.dat). These files contain data for a simulation period from January 1, 1940, to September 30, 2006, and should not be modified. Any variable can be output by modifying the code to write data from the salsolve program to a subfolder called "outputs". Spin up time for the model to become insensitive to initial sediment bed elevations is around 10 years of simulation (Schoellhamer and others, 2008). The time required to simulate 65 years is less than 10 minutes on a desktop personal computer. While the model is running, a screen counting down the number of time steps remaining in the simulation is displayed.

Applications of the Sediment-Transport Model

The sediment-transport model described in this report has been used to develop sediment budgets of the Bay (Schoellhamer and others, 2005), estimate geomorphic effects of wetland restoration on South San Francisco Bay mudflats (May and others, 2005), and track sediment-bound contaminants such as PCBs (Oram and Davis, 2008; Oram and others, 2008).

Table 5. Percent change in suspended-sediment concentration, relative to a 20-percent increase of each calibration coefficient for the sediment model calibrated to suspended-sediment concentrations.

Subembayment	+20% c_D		+20% c_E		+20% c_W	
	Upper	Lower	Upper	Lower	Upper	Lower
Suisun Bay (percent change)	–14	2	10	13	5	7
San Pablo Bay (percent change)	–11	20	7	5	3	8
Central Bay (percent change)	–15	–6	11	12	4	3
South Bay (percent change)	–19	10	19	25	15	32

Table 6. Percent change in net sedimentation, relative to a 20-percent increase of each calibration coefficient for the sediment model calibrated to net sedimentation.

Subembayment	+20 percent c_D	+20 percent c_E	+20 percent c_W
Suisun Bay (percent change)	34	–30	0.1
San Pablo Bay (percent change)	13	–50	–30
South Bay (percent change)	21	–23	–3

Conclusions

This report describes a simple tidally averaged box model of sediment transport in San Francisco Bay. A sediment model was added to the Uncles–Peterson (1995) salinity model. The salinity model was validated by comparing simulated salinity with continuous salinity data collected in water year 1999. Model simulations under-predicted salinity in North Bay and slightly over-predicted salinity in South and Central Bays. Overall, the model was able to predict the salinity field reasonably throughout the Bay indicating that longitudinal and vertical mixing on an inter-tidal time scale is well defined. The sediment model was calibrated to measured SSC, but this model poorly hindcast net sedimentation. The model was recalibrated to hindcast net sedimentation calculated from bathymetric change data. Calibration to net-basin sedimentation caused the shallows to erode while channels deposited because model surface-layer boxes span both shallows and channel and neglect lateral variability of SSC. Validation with recent (1983–2005) net sedimentation in South San Francisco Bay was poor, perhaps due to poorly quantified sediment supply and invasive species that altered erosion and deposition processes. This demonstrates the difficulty of predicting future sedimentation. The model would best be used as a tool for developing past and present sediment budgets, and for creating scenarios of future sedimentation that are compared to one another rather than considered a deterministic prediction.

Acknowledgments

Funding for model development was provided by the San Francisco Bay Regional Water Quality Control Board and the U.S. Geological Survey California Federal/State Cooperative Program. Additional funding to write this report was provided by the Clean Estuary Partnership of the Bay Area Clean Water Agencies and the U.S. Geological Survey Federal/State Cooperative Program.

References Cited

Alpine, A.E., and Cloern, J.E., 1992, Trophic interactions and direct physical effects control phytoplankton biomass and production in an estuary: Limnology and Oceanography, v. 37, no. 5, p. 946–955.

Arzayus, K.M., Dickhut, R.M., and Canuel, E.A., 2002, Effects of physical mixing on the attenuation of polycyclic aromatic hydrocarbons in estuarine sediments: Organic Geochemistry, v. 33, p. 1759–1769.

Bergamaschi, B.A., Kuivila, K.M., and Fram, M.S., 2001, Pesticides associated with suspended sediments entering San Francisco Bay following the first major storm of water year 1996: Estuaries, v. 24, no. 3, p. 368–380.

Bindoff, N.L., Willebrand, J., Artale, V., Cazenave, A., Gregory, J., Gulev, S., Hanawa, K., Le Quéré, C., Levitus, S., Nojiri, Y., Shum, C.K., Talley, L.D., and Unnikrishnan, A., 2007, Observations: oceanic climate change and sea level, *in* Solomon, S., Qin, D., Manning, M., Chen, Z., Marquis, M., Averyt, K.B., Tignor, M., and Miller, H.L. (eds.), Climate change 2007: The physical science basis. Contribution of Working Group I to the Fourth Assessment Report of the Intergovernmental Panel on Climate Change: Cambridge, Cambridge University Press, United Kingdom and New York.

Buchanan, P.A., 2000, Specific conductance, water temperature, and water level data, San Francisco Bay, California, water year 1999: Interagency Ecological Program Newsletter, v. 13, no. 3, p. 17–20. URL *http://www.iep.ca.gov/report/newsletter/*

Buchanan, P.A., and Ruhl, C.A., 2001, Summary of suspended-sediment concentration data, San Francisco Bay, California, water year 1999: U.S. Geological Survey Open-File Report 01–100, 41 p.

Caffrey, J.M., 1995, Spatial and seasonal patterns in sediment nitrogen remineralization and ammonium concentrations in San Francisco Bay, California: Estuaries, v. 18, no. 1B, p. 219–233.

California Department of Water Resources, 1986, DAYFLOW program documentation and DAYFLOW summary user's guide. URL *http://www.iep.ca.gov/dayflow/index.html*

Cappiella, Karen, Malzone, Chris, Smith, R.E., and Jaffe, B.E., 1999, Sedimentation and bathymetry changes in Suisun Bay, 1867–1990: U.S. Geological Survey Open-File Report 99-563, 1 p., poster.

Choe, K.-Y., Gill, G.A., and Lehman, R., 2003, Distribution of particulate, colloidal, and dissolved mercury in San Francisco Bay estuary. I. Total mercury: Limnology and Oceanography, v. 48, no. 4, p. 1535–1546.

Conaway, C.H., Squire, S., Mason, R.P., and Flegal, A.R., 2003, Mercury speciation in the San Francisco Bay estuary: Marine Chemistry, v. 80, p. 199–225.

Conomos, T.J., 1979, Properties and circulation of San Francisco Bay waters, *in* Conomos, T.J. (ed.), San Francisco Bay, The Urbanized Estuary: San Francisco, California, Pacific Division of the American Association for the Advancement of Science, p. 47–84.

Conomos, T.J., and Peterson, D.H., 1977, Suspended-particle transport and circulation in San Francisco Bay, an overview: New York, Estuarine Processes, Academic Press, v. 2, p. 82–97.

Dettinger, M.D., Cayan, D.R., Meyer, M.K., and Jeton, A.E., 2004, Simulated hydrologic responses to climate variations and change in the Merced, Carson, and American River Basins, Sierra Nevada, California, 1900–2099: Climate Change, v. 62, p. 283–317.

Fischer, H.B., List, E.J., Koh, R.C.Y., Imberger, J., and Brooks, N.H., 1979, Mixing in inland and coastal waters: New York, Academic Press.

Flick, R.E., Murray, J.F., and Ewing, L.C., 2003, Trends in United States tidal datum statistics and tide range: Journal of Waterway, Port, Coastal and Ocean Engineering, v. 129, no. 4, p. 155–164.

Foxgrover, A.C., Jaffe, B.E., Hovis, G.T., Martin, C.A., Hubbard, J.R., Samant, M.R., and Sullivan, S.M., 2007, 2005 hydrographic survey of south San Francisco Bay, California: U.S. Geological Survey Open-File Report 2007–1169, 113 p.

Foxgrover, A.C., Higgins, S.A., Ingraca, M.K., Jaffe., B.E., and Smith, R.E., 2004, Deposition, erosion, and bathymetric change in South San Francisco Bay: 1858–1983: U.S. Geologic Survey, Open-File Report 2004–1192, 25 p.

Gleick, P.H., 1987, The development and testing of a water balance model for climate impact assessment: Modeling the Sacramento Basin: Water Resources Research v. 23, p. 1049–1061.

Gleick, P.H. and Chalecki, E.L, 1999, The impacts of climatic changes for water resources of the Colorado and Sacramento–San Joaquin River Basins: Journal of American Water Resources Association, v. 35, p. 1429–1441.

Goals Project, 1999, Baylands ecosystem habitat goals. A report of habitat recommendations prepared by the San Francisco Bay Area Wetlands Ecosystem Goals Project: Oakland, Calif, U.S. Environmental Protection Agency, San Francisco, California/S.F. Bay Regional Water Quality Control Board.

Goodwin, P., and Denton, R.A., 1991, Seasonal influences on the sediment transport characteristics of the Sacramento River: Proceedings Institution of Civil Engineers, part 2, v. 91, p. 163–172.

Hayter, E.J., 1984, Estuarial sediment bed model, *in* A.J. Mehta, (ed.), Lecture notes on coastal and estuarine studies, 14: Estuarine Cohesive Sediment Dynamics, p. 326–359.

Hood, W.G., 2004, Indirect environmental effects of dikes on estuarine tidal channels: thinking outside of the dike for habitat restoration and monitoring: Estuaries, v. 27, no. 2, p. 273–282.

Hornberger, M.I., Luoma, S.N., van Geen, A., Fuller, C., and Anima, R., 1999, Historical trends of metals in the sediments of San Francisco Bay, California: Marine Chemistry, v. 64, p. 39–55.

Jaffe, B.E., Smith, R.E, and Zink Torresan, L., 1998, Sedimentation and bathymetric change in San Pablo Bay 1856–1983: U.S. Geological Survey Open-File Report 98–0759, 1 sheet.

Jeton, A.E., Dettinger, M.D., and Smith, J.L., 1996, Potential effects of climate change on streamflow, eastern and western slopes of the Sierra Nevada, California, and Nevada: U.S. Geological Survey Water-Resources Investigations Report 95–4260, 44 p.

Kamphius, J.W., 1975, Friction factor under oscillatory waves: Journal of the Waterways, Harbors, and Coastal Engineering Division, ASCE, v. 101, no. WW2, p. 135–144.

Kimmerer, W.J., Gartside, E., and Orsi, J.J., 1994, Predation by an introduced clam as the likely cause of substantial declines in zooplankton of San Francisco Bay: Marine Ecology Progress Series, v. 113, p. 81–93.

Kirby, R., 1990, The sediment budget of the erosional intertidal zone of the Medway Estuary, Kent: Proceedings of the Geological Association, v. 101, no. 1. p. 63–77.

Knowles, Noah, 1996, Simulation and prediction of salinity variability in San Francisco Bay: La Jolla, California, University of California, San Diego, Scripps Institution of Oceanography, master's thesis.

Knowles, Noah, 2000, Modeling the hydroclimate of the San Francisco Bay–Delta estuary and watershed: San Diego, University of California, Ph.D. Dissertation.

Knowles, Noah, 2002, Natural and human influences on freshwater inflows and salinity in the San Francisco estuary at monthly to interannual scales: Water Resources Research, v. 38, no. 12, doi:10.1029/2001WR000360.

Knowles, Noah and Cayan, D.R., 2002, Potential effects of global warming on the Sacramento/San Joaquin watershed and the San Francisco estuary: Geophysical Research Letters, v. 29, no. 18, doi:10.1029/2001GL014339.

Knowles, Noah and Cayan, D.R., 2004, Elevational dependence of projected hydrologic changes in the San Francisco estuary and watershed: Climatic Change, v. 62, p. 319–336.

Krone, R.B., 1979, Sedimentation in the San Francisco Bay system, *in* Conomos, T.J. (ed.), San Francisco Bay: The Urbanized Estuary. Pacific Division of the American Association for the Advancement of Science, San Francisco, California, p. 85–96.

Krone, R.B., 1999, Effects of bed structure on erosion of cohesive sediments: Journal of Hydraulic Engineering, ASCE, v. 125, no. 12, p. 1297–1301.

Lee, S.V., and Cundy, A.B., 2001, Heavy metal contamination and mixing processes in sediments from the Humber Estuary, Eastern England: Estuarine, Coastal and Shelf Science, v. 53, p. 619–636.

Le Roux, S.M., Turner, A., Millward, G.E., Ebdon, L., and Apprion, P., 2001, Partitioning of mercury onto suspended sediments in estuaries: Journal of Environmental Monitoring, v. 3, p. 37–42.

Lettenmaier, D.P., and Gan, T.Y., 1990, Hydrologic sensitivities of the Sacramento–San Joaquin River Basin, California, to Global Warming: Water Resources Research, v. 26, p. 69–86.

Lionberger, M.A., 2003, A tidally averaged sediment-transport model of San Francisco Bay, California: Master's thesis, The University of California, Davis.

McDonald, E.T., and Cheng, R.T, 1997, A numerical model of sediment transport applied to San Francisco Bay, California: Journal of Marine Environmental Engineering, v. 4, p. 1–41.

May, C., Lionberger, M., Williams, P., Schoellhamer, D., Misra, G., Orr, M., and Ritchie, S., 2005, Landscape-scale geomorphic effects of wetland restoration associated with the South Bay salt pond restoration project: Proceedings of the 7th biennial State-of-the-Estuary Conference, Oakland, California, October 4–6, 2005, p. 139.

McKee, L.J., Ganju, N.K., Schoellhamer, D.H., 2006, Estimates of suspended sediment flux entering San Francisco Bay from the Sacramento and San Joaquin Delta, San Francisco Bay, California: Journal of Hydrology, v. 323, p. 335–352.

Meyer-Peter, E., and Mueller, R., 1948, Formulas for bed-load transport: Report on second meeting of the International Association for Hydraulic Research, Stockholm, Sweden, p. 39–64.

Munk, W.H., and Anderson, E.R., 1948, Note on the theory of the thermocline: Journal of Marine Research, v. 7, p. 276–295.

Nichols, F.H., and Thompson, J.K., 1985, Time scales of change in the San Francisco Bay benthos: Hydrobiologia, v. 192, p. 121–138.

Nichols, F.H., Thompson, J.K., and Schemel, L.E., 1990, Remarkable invasion of San Francisco Bay (California, USA) by the Asian clam Potamocorbula amurensis. II. Displacement of a former community: Marine Ecology Progress Series, v. 66, p. 95–101.

Officer, C.B., 1976, Physical oceanography of estuaries (and associated coastal waters): New York, John Wiley and Sons.

Ogden Beeman and Associates and Ray B. Krone and Associates, 1992, Sediment budget study for San Francisco Bay: Final report prepared for the San Francisco District, U.S. Army Corps of Engineers.

Okubo, A., 1973, Effect of shoreline irregularities on streamwise dispersion in estuaries and other embayments: Netherlands Journal of Sea Research, v. 6, p. 213–224.

Oram, J.J., Davis, J.A., and Leatherbarrow, J.E., 2008, A Model of Long-Term PCB Fate in San Francisco Bay: Model Formulation, Calibration, and Uncertainty Analysis (v 2.1): Oakland, California, Regional Monitoring Program Technical Report, San Francisco Estuary Institute.

Oram, J.J., and Davis, J.A. 2008, A forecast model of long-term PCB fate in San Francisco Bay: Oakland, California, Regional Monitoring Program Technical Report, San Francisco Estuary Institute.

Oros, D.R., Hoover, D., Rodigari, F., Crane, D., and Sericano, J., 2005, Levels and distribution of polybrominated diphenyl ethers in water, surface sediments, and bivalves from the San Francisco Estuary: Environmental Science and Technology, v. 39, no. 1, p. 33–41.

Poland, J.F. and Ireland, R.L., 1988, Land subsidence in the Santa Clara Valley, California, as of 1982: U.S. Geological Survey Professional Paper, 497-F.

Porterfield, G., 1980, Sediment transport of streams tributary to San Francisco, San Pablo, and Suisun Bays, California, 1909–66: U.S. Geological Survey Water-Resources Investigations Report 80–64, 92 p.

Ridgeway, J., and Shimmield, G., 2002, Estuaries as repositories of historical contamination and their impact on shelf seas: Estuarine, Coastal and Shelf Science, v. 55, p. 903–928.

Roos, M., 1989, Possible climate change and its impact on water supply in California: Seattle, Washington, Oceans '89 Conference, September 18–21, 1989.

Ross, J.R.M., and Oros, D.R., 2004, Polycyclic aromatic hydrocarbons in the San Francisco Estuary water column: sources, spatial distributions, and temporal trends (1993–2001): Chemosphere, v. 57, p. 909–920.

Rudnick, D.A., Chan, V., and Resh, V.H., 2005, Morphology and impacts of the burrows of the Chinese mitten crab, Eriocheir sinensis H. Milne Edwards (Decapoda, grapsoidea), in South San Francisco Bay, California, U.S.A.: Crustaceana, v. 78, no. 7, p. 787–807.

Ruhl, C.A., and Schoellhamer, D.H., 2004, Spatial and temporal variability of suspended-sediment concentrations in a shallow estuarine environment: San Francisco Estuary and Watershed Science, v. 2, no. 2, article 1. URL *http://repositories.cdlib.org/jmie/sfews/vol2/iss2/art1*

Ruhl, C.A., Schoellhamer, D.H., Stumpf, R.P., and Lindsay, C.L., 2001, Combined use of remote sensing and continuous monitoring to analyse the variability of suspended-sediment concentrations in San Francisco Bay, California: Estuarine, Coastal, and Shelf Science, v. 53, p. 801–812.

Sanudo–Wilhelmy, S.A., Rivera-Duarte, I., and Flegal, A.R., 1996, Distribution of colloidal trace metals in the San Francisco Bay estuary: Geochimica et Cosmochimica Acta, v. 60, no. 24, p. 4933–4944.

Schoellhamer, D.H., 1996, Factors affecting suspended-solids concentrations in South San Francisco Bay, California: Journal of Geophysical Research, v. 101, no. C5, p. 12087–12095.

Schoellhamer, D.H., 2002, Variability of suspended-sediment concentration at tidal to annual time scales in San Francisco Bay, USA: Continental Shelf Research, v. 22, p. 1857–1866.

Schoellhamer, D.H., Ganju, N.K., Mineart, P.R., and Lionberger, M.A., 2008, Sensitivity and spin up times of cohesive sediment-transport models used to simulate bathymetric change, *in* Kusuda, T., Yamanishi, H., Spearman, J., and Gailani, J.Z., (ed.), Sediment and ecohydraulics: Elsevier Science B.V., p. 463–476.

Schoellhamer, D.H., Lionberger, M.A., Jaffe, B.E., Ganju, N.K., Wright, S.A., and Shellenbarger, G.G., 2005, Bay sediment budgets: Sediment accounting 101: The pulse of the estuary: Monitoring and managing water quality in the San Francisco Estuary: Oakland, California, San Francisco Estuary Institute, p. 58–63.

Schoellhamer, D.H., Mumley, T., and Leatherbarrow, J.E., 2007, Suspended sediment and sediment-associated contaminants in San Francisco Bay: Environmental Research, v. 105, p. 119–131.

Schoellhamer, D.H., Orlando, J.L., Wright, S.A., and Freeman, L.A., 2006, Sediment supply and demand: Proceedings of the South Bay Science Symposium, June 6, 2006, San Jose, California, p. 3. *http://www.southbayrestoration.org/pdf_files/science%20symposium/2006%20Science%20Symposium%20Poster%20Abstracts.pdf*

Snyder, M.A., Bell, J.L., Sloan, L.C., Duffy, P.B., and Govindasamy, B., 2002, Climate responses to a doubling of atmospheric carbon dioxide for a climatically vulnerable region: Geophysical Research Letters, v. 29, no. 11, doi:10.1029/2001GL014431.

Sternberg, R.W., Cacchione, D.A., Drake, D.E., and Kranck, K., 1986, Suspended sediment transport in an estuarine tidal channel within San Francisco Bay, California: Marine Geology, v. 71, p. 237–258.

Sturm, T.W., 2001, Open channel hydraulics: first edition, McGraw-Hill series in water resources and environmental engineering: New York, McGraw-Hill.

Swanson, K., Shellenbarger, G.G., Schoellhamer, D.H., Ganju, N.K., Athearn, N., and Buchanan, P., 2003, Desalinization, erosion, and tidal changes following the breaching of Napa salt pond 3: Oakland, California, Proceedings of the 6th biennial State-of-the-Estuary Conference, October 21–23, 2003, p. 156.

Taylor, S.E., Birch, G.F., and Links, F., 2004, Historical catchment changes and temporal impact on sediment of the receiving basin, Port Jackson, New South Wales: Australian Journal of Earth Sciences, v. 51, p. 233–246.

Thompson, J.K., 2005, One estuary, one invasion, two responses: Phytoplankton and benthic community dynamics determine the effect of an estuarine invasive suspension-feeder, *in* Dame, R.F. and Olenin, S., (eds.), The comparative roles of suspension-feeders in ecosystems: Springer, p. 291–316.

Turner, A., Hyde, T.L., and Rawling, M.C., 1999, Transport and retention of hydrophobic organic micropollutants in estuaries: implications of the particle concentration effect: Estuarine, Coastal and Shelf Science, v. 49, p. 733–746.

Turner, A., and Millward, G.E., 2000, Particle dynamics and trace metal reactivity in estuarine plumes: Estuarine, Coastal and Shelf Science, v. 50, p. 761–774.

Turner, A., and Millward, G.E., 2002, Suspended particles: their role in estuarine biogeochemical cycles: Estuarine, Coastal and Shelf Science, v. 55, p. 857–883.

Uncles, R.J., 1991, M4 tides in a macrotidal, vertically mixed estuary: the Bristol Channel and Severn: Tidal Hydrodynamics, B. Parker, Wiley, p. 341–356.

Uncles, R.J., 2003, From catchment to coastal zone: examples of the application of models to some long-term problems: The Science of the Total Environment, v. 314–316, p. 567–588.

Uncles, R.J., and Joint, I.R., 1983, Vertical mixing and its effects on phytoplankton growth in a turbid estuary: Canadian Journal of Fisheries and Aquatic Science, v. 40, p. 221–228.

Uncles, R.J., and Peterson, D.H., 1995, A computer model of long-term salinity in San Francisco Bay: sensitivity to mixing and inflows: Environment International, v. 21, no. 5, p. 647–656.

Uncles, R.J., and Peterson, D.H., 1996, The long-term salinity field in San Francisco Bay: Continental Shelf Research, v. 16, p. 2005–2039.

Venkatesan, M.I., de Leon, R.P., van Geen, A., and Luoma, S.N., 1999, Chlorinated hydrocarbon pesticides and polychlorinated biphenyls in sediment cores from San Francisco Bay: Marine Chemistry, v. 64, p. 85–97.

Warner, J.C., Schoellhamer, D.H., Ruhl, C.A., and Burau, J.R., 2004, Floodtide pulses after low tides in shallow subembayments adjacent to deep channels: Estuarine, Coastal and Shelf Science, v. 60, no. 2, p. 213–228.

Widdows, J., Blauw, A., Heip, C.H.R., Herman, P.M.J., Lucas, C.H., Middelburg, J.J., Schmidt, S., Brinsley, M.D., Twisk, F., and Verbeek, H., 2004, Role of physical and biological processes in sediment dynamics of a tidal flat in Westerschelde Estuary, SW Netherlands: Marine Ecology Progress Series, v. 274, p. 41–56.

Wright, S.A., and Schoellhamer, D.H., 2004, Trends in the sediment yield of the Sacramento River, California, 1957–2001: San Francisco Estuary and Watershed Science. v. 2, no. 2, article 2.

Wright, S.A., and Schoellhamer, D.H., 2005, Estimating sediment budgets at the interface between rivers and estuaries with application to the Sacramento–San Joaquin River Delta: Water Resources Research, v. 41, W09428, doi:10.1029/2004WR003753.

Appendix

Table A1. Calibration coefficients for the sediment-transport model calibrated to suspended-sediment concentration.

Box	c_D	c_E	c_W
1	0.00004	0.000008	0.005
2	.00004	.000008	.005
3	.00004	.000008	.005
4	.00004	.000008	.005
5	.00004	.000008	.005
6	.00004	.000008	.005
7	.00004	.000008	.005
8	.00004	.000008	.005
9	.00004	.000008	.005
10	.00004	.000008	.005
11	.00004	.000008	.005
12	.00004	.000008	.005
13	.00004	.000008	.005
14	.00004	.000008	.005
15	.00004	.00004	.005
16	.00004	.00004	.005
17	.00004	.00004	.005
18	.00004	.00004	.005
19	.00004	.00004	.005
20	.00004	.00004	.005
21	.00004	.00004	.005
22	.00004	.00004	.005
23	.00004	.00004	.005
24	.00004	.00004	.005
25	.00004	.00004	.005
26	.00004	.00004	.005
27	.00004	.00004	.005
28	.00004	.00004	.005
29	.00004	.00004	.005
30	.00004	.00004	.005
31	.00004	.00004	.005
32	.00004	.00004	.005
33	.00004	.00004	.005
34	.00004	.00004	.005
35	.00004	.00004	.005
36	.00004	.00004	.005
37	.00004	.00004	.005
38	.00004	.00004	.005
39	.00004	.00004	.005
40	.00004	.00004	.005
41	.00004	.00004	.005
42	.00004	.00004	.005
43	.00004	.00004	.005
44	.00004	.00004	.005
45	.00004	.00004	.005
46	.00004	.00004	.005
47	.00004	.00004	.005
48	.00004	.00004	.005
49	.00004	.00004	.005
50	.00004	.00004	.005
51	.00004	.00004	.005

Table A2. Calibration coefficients for the sediment-transport model calibrated to net change in sediment storage.

Box	c_D	c_E	c_W
1	0.0001	0.000353	0.0001
2	.0001	.000353	.0001
3	.0001	.000353	.0001
4	.0001	.000353	.0001
5	.0001	.0003487	.0001
6	.0001	.0003487	.0001
7	.0001	.0003487	.0001
8	.0001	.0003487	.0001
9	.0001	.0004425	.0001
10	.0001	.0004425	.0001
11	.0001	.0004425	.0001
12	.0001	.0002658	.0001
13	.0001	.0002658	.0001
14	.0001	.0002658	.0001
15	.0001	.0000502	.0001
16	.0001	.0000502	.0001
17	.0001	.0000502	.0001
18	.0001	.0000502	.0001
19	.0001	.0000502	.0001
20	.0001	.0000502	.0001
21	.0001	.0000502	.0001
22	.0001	.0000502	.0001
23	.0001	.0000676	.0001
24	.0001	.0000676	.0001
25	.0001	.0000676	.0001
26	.0001	.0000676	.0001
27	.0001	.0000676	.0001
28	.0001	.0000676	.0001
29	.0001	.000344	.0001
30	.0001	.000344	.0001
31	.0001	.000344	.0001
32	.0001	.000344	.0001
33	.0001	.000344	.0001
34	.0001	.000344	.0001
35	.0001	.000344	.0001
36	.0001	.000344	.0001
37	.0001	.000344	.0001
38	.0001	.000344	.0001
39	.0001	.000344	.0001
40	.0001	.000344	.0001
41	.0001	.000344	.0001
42	.0001	.000344	.0001
43	.0001	.000344	.0001
44	.0001	.000344	.0001
45	.0001	.000344	.0001
46	.0001	.0000502	.0001
47	.0001	.0000502	.0001
48	.0001	.0000502	.0001
49	.0001	.0000502	.0001
50	.0001	.0000502	.0001
51	.0001	.0000502	.0001